JOURNAL OF GEOPHYSICAL RESEARCH, VOL. 112, B06103, doi:10.1029/2006JB004699, 2007

Origin of orogenic remagnetizations in Mississippian carbonates, Sawtooth Range, Montana

V. J. O'Brien,[1] K. M. Moreland,[1] R. D. Elmore,[1] M. H. Engel,[1] and M. A. Evans[2]

Received 15 August 2006; revised 12 January 2007; accepted 9 February 2007; published 23 June 2007.

[1] Paleomagnetic results are presented from Mississippian Madison Group carbonates in the Sawtooth Range, northwestern Montana. Samples were collected from sites along two east-west trending transects perpendicular to the thrust faults in the Sun River Canyon and in the North and South Forks of the Teton River and from three folds. The Madison Group contains a widespread characteristic remanent magnetization (ChRM) that resides in magnetite with southerly declinations and moderately steep up inclinations. Tilt test results suggest that the ChRM is pretilting in the thrust sheets and Teton anticline but syntilting in the Clary Coulee and Swift Dam folds. The ChRMs all have the same characteristics and were probably caused by the same remagnetization event, yet the tilt test results are different. One explanation involves the difference in fold types between the Teton anticline (fault bend fold geometry) and the Clary Coulee and Swift Dam folds (fault propagation fold geometries). The deformation that produced the two geometries could have caused variations in strain/stress, which may have altered an original pretilting into a syntilting ChRM. A mean paleopole for the three pretilting tilt test results (67.2°N, 177.9°E; A_{95} = 13.1°) suggests remanence acquisition in the late Jurassic–early Tertiary. The ChRM is interpreted as a chemical remanent magnetization (CRM). Geochemical studies indicate that the Mississippian carbonates were altered by evolved fluids with radiogenic $^{87}Sr/^{86}Sr$ values, and petrographic analysis indicates that hydrocarbons migrated through the carbonates. The CRM is interpreted to be related to alteration by one of these fluids.

Citation: O'Brien, V. J., K. M. Moreland, R. D. Elmore, M. H. Engel, and M. A. Evans (2007), Origin of orogenic remagnetizations in Mississippian carbonates, Sawtooth Range, Montana, *J. Geophys. Res.*, *112*, B06103, doi:10.1029/2006JB004699.

1. Introduction

[2] Secondary chemical remanent magnetizations (CRMs) are common in Paleozoic carbonate rocks from mountain belts in North America [e.g., *Enkin et al.*, 2000; *Blumstein et al.*, 2004]. Many of these CRMs were acquired about the time of deformation and are termed orogenic remagnetizations [*Enkin et al.*, 2000], but their origins are not completely understood. Previous studies have related some orogenic remagnetizations to externally derived fluids such as hydrocarbons or other fluids that were activated as a result of orogenesis [*McCabe and Elmore*, 1989; *Oliver*, 1992]. Other CRMs have been related to burial diagenetic processes such as clay diagenesis [*Katz et al.*, 2000] and/or hydrocarbon maturation [*Blumstein et al.*, 2004]. In addition, some studies have reported that orogenic remagnetizations occur in trends parallel to the shortening direction in the Canadian Cordillera [*Enkin et al.*, 2000]. Understanding the origin of these CRMs is important because they provide the opportunity to date fluid migration and burial diagenetic events.

[3] Many orogenic CRMs are apparently syntilting (i.e., acquired during the folding or tilting event). A number of authors suspect that some of the syntilting CRMs may actually be pretilting magnetizations that have been altered due to strain and/or stress during deformation [e.g., *Kligfield et al.*, 1983; *Hirt et al.*, 1986; *Cogne and Perroud*, 1987; *van der Pluijm*, 1987; *Kodama*, 1988; *Hudson et al.*, 1989; *Stamatakos and Kodama*, 1991a, 1991b; *Stamatakos and Hirt*, 1994; *Borradaile*, 1997; *Lewchuk et al.*, 2003; *Elmore et al.*, 2006]. For example, strain may cause syntilting remagnetizations through rotation of remanence carrying grains during deformation. It is important to resolve this issue because true timing of remagnetization needs to be known when using paleomagnetism to date diagenetic events. It is also important to know the true timing of remagnetization when addressing tectonic problems [e.g., *Miller and Kent*, 1986; *Kent*, 1988; *Stamatakos et al.*, 1996; *Van der Voo et al.*, 1997; *Aubourg and Chabert-Pelline*, 1999].

[4] The primary objective of this study is to investigate the origin(s) and timing of widespread orogenic remagnetizations in the Madison Group carbonates that form part of the thrust and fold belt in the Sawtooth Range, Montana (Figure 1). A second objective is to compare tilt test results

[1] School of Geology and Geophysics, University of Oklahoma, Norman, Oklahoma, USA.
[2] Department of Physics and Earth Sciences, Central Connecticut State University, New Britain, Connecticut, USA.

0148-0227/07/2006JB004699$09.00

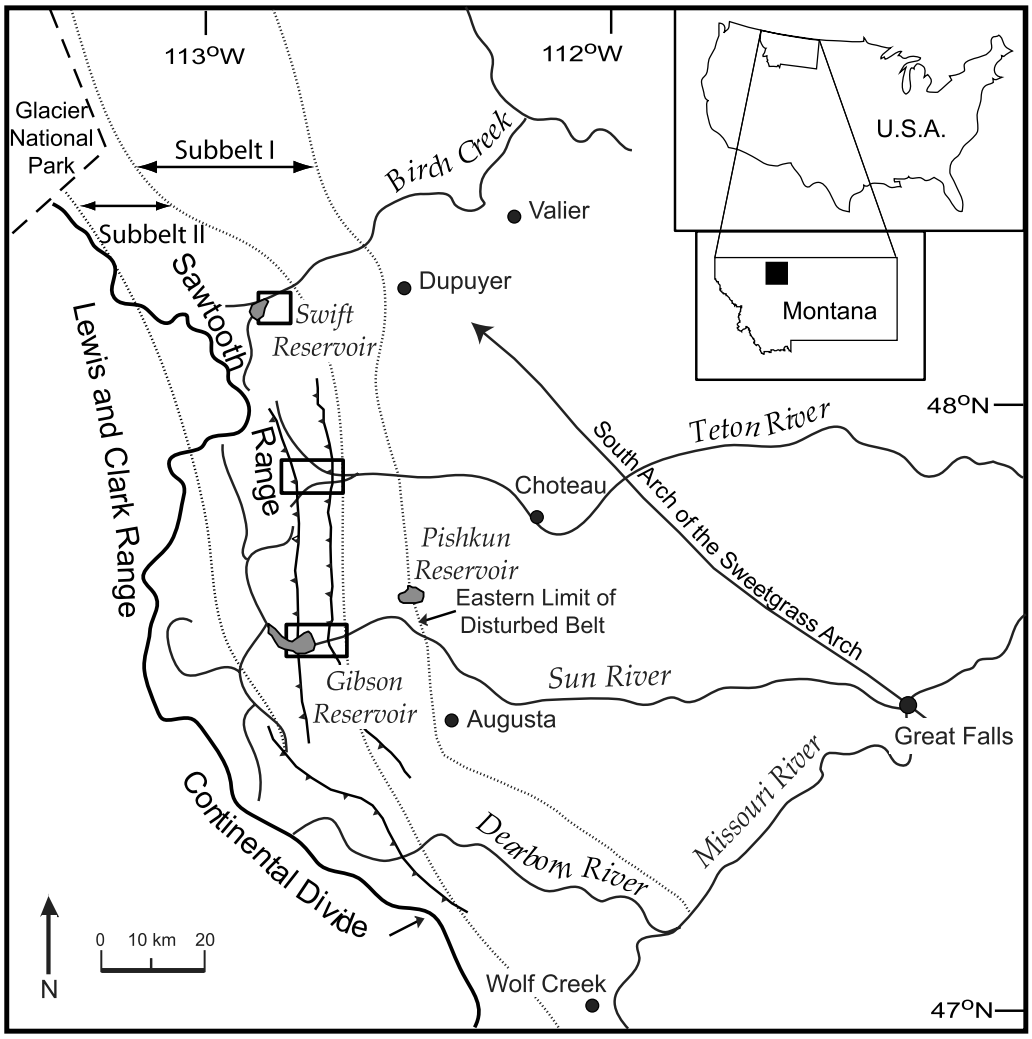

Figure 1. Location map of study area in northwest Montana with inset maps of Montana and the United States (modified from *Mudge* [1972]). Samples were collected from the Sawtooth Range, which lies in the northern disturbed belt. Areas in boxes represent the three main sampling locations from Swift Reservoir in the north to the North and South Forks of the Teton River in the center region to Sun River Canyon in the south. Dashed lines outline the subbelts as delineated by *Mudge* [1982]. Corresponding geologic maps for each of the boxed areas are given in Figures 2a–2c.

from different types of fold geometries (fault bend and fault propagation) and from carbonate units tilted by thrust faults to test if there are differences that may help understand the origin of syntilting CRMs. A third objective is to test for remagnetization trends similar to those reported by other workers in the Canadian Cordillera [e.g., *Enkin et al.*, 2000].

[5] These objectives were met by sampling carbonates from the major thrust sheets along several east-west trending transects perpendicular to the mountain front and three folds (Figure 2). Seven major thrust sheets were sampled in the Sun River Canyon and five major thrust sheets in the North and South Forks of the Teton River. Samples were also collected from two folds with fault propagation geometries (Swift Dam fold and a small fold along the North Fork of the Teton River at Clary Coulee) and the Teton anticline, a fold with fault bend geometry. Preliminary results from the thrust sheets and Clary Coulee fold are presented in the work of *O'Brien et al.* [2006]. Tilt tests were performed to constrain the timing of remagnetization. In addition, rock magnetic, petrographic, and geochemical analyses were conducted on the limestones and dolostones to aid in determining the origin(s) of the remagnetizations.

2. Geologic Setting

[6] The fold and thrust belt of the Sawtooth Range is located in northwestern Montana (Figure 1). The study area is ~90 km west of Great Falls, Montana, and ~75 km south of Glacier National Park. The field area extends from the Sun River Canyon in the south to the North and South Forks of the Teton River, and finally to the Swift Reservoir in the north. The Sawtooth Range is one of many ranges that make up the northern disturbed belt (also known as the Montana disturbed belt), which lies ~20 km to the west of the eastern limit of the disturbed belt. The northern disturbed belt is part of the North American Cordillera that extends from Alaska to Mexico and includes the Canadian Cordillera. In the study area, the disturbed belt consists of a succession of

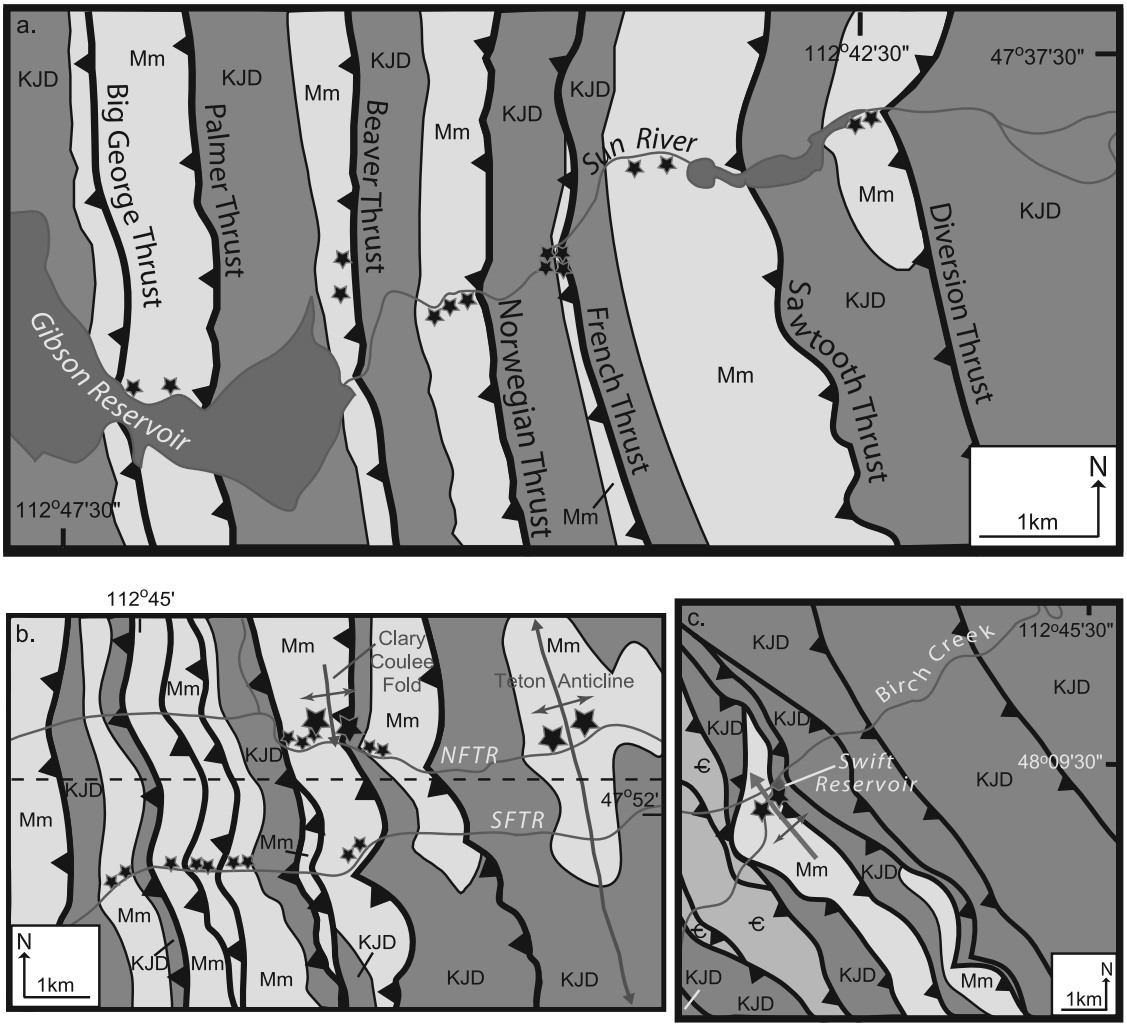

Figure 2. (a) Geologic map of the thrust sheets along the Sun River (modified from *Mudge* [1972]). Sample locations in the Madison Group (Mm) that are included in the tilt tests are represented by stars. Each star represents approximately seven to nine specimens. The valleys between the carbonate units contain Cretaceous, Jurassic, and Devonian clastics (KJD). (b) Geologic map of the thrust sheets and folds along the North and South Forks of the Teton River (modified from *Mudge and Earhart* [1983]). Dashed line shows position of cross section in Figure 3. Larger stars represent between 4 and 15 site locations on each limb of the folds: Clary Coulee and Teton anticlines. NFTR, North Fork of the Teton River; SFTR, South Fork of the Teton River. (c) Geologic map of Swift Dam fold (modified from *Mudge and Earhart* [1983]). Cambrian units (C) reside to the west of the sample area.

westerly dipping, imbricate thrust sheets and folds that trend approximately north–south (Figure 3). The Sawtooth Range is arranged in an anastomosing series of thrust sheets that diverge from a westward dipping sole detachment fault [*Lageson*, 1987]. On the basis of structural style, *Mudge* [1972] subdivided the region from east to west into subbelts I through IV, respectively. The part of the Sawtooth Range in this study lies in subbelt II (Figure 1). Subbelt II is approximately 100 km long by 20 km wide and encompasses the series of thrust sheets and folds in Mesozoic and Paleozoic rocks [*Mudge*, 1972].

[7] The majority of the structures in the region are a product of the Laramide orogeny (~75–51 Ma) [e.g., *Burchfiel et al.*, 1992], which produced deformation and shortening that resulted in the eastward propagating thrust sheets and folds. Potassium-argon (K-Ar) dating of diagenetic clays caused by deformation in Cretaceous bentonites suggests that the timing of deformation of the Sawtooth Range is approximately 72–56 Ma [*Hoffman et al.*, 1976]. *Mudge* [1982] suggests that the majority of the deformation in the Sawtooth Range occurred during Paleocene time. These thrust sheets juxtaposed Mississippian Madison Group carbonates atop Cretaceous shales (and sandstones) and Devonian carbonates. In this study, the thrust sheets (Figure 4a) have dips ranging from 24° to 79°W with the shallowest dips in the eastern thrust sheets (i.e., Diversion) and the steepest dips in the western thrust sheets (i.e., Big George).

[8] Excellent exposures of the Mississippian Madison Group occur within the study area, thus it was the lithology sampled. The Madison Group (Figure 5) consists of the older Allan Mountain Limestone (Kinderhookian to Osagean) and the younger Castle Reef Dolomite (Osagean to Meramecian)

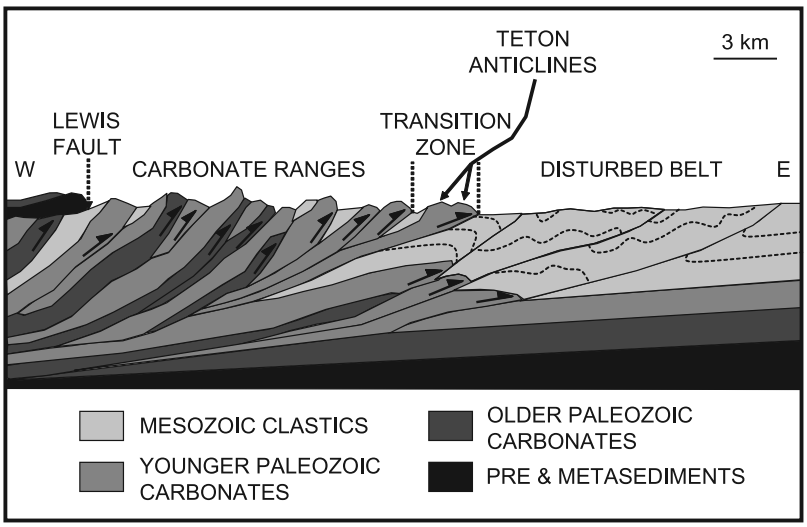

Figure 3. Schematic cross section of typical Sawtooth thrust faulting. "Teton anticlines" refer to both Teton Main and Teton East. Teton Main is the Teton anticline of this study (provided by D. W. Stearns, University of Oklahoma, 2005). Approximate line of cross section is shown in Figure 2b.

[*Mudge*, 1972]. The Allan Mountain Limestone ranges in thickness from approximately 160 to 185 m and consists of medium to dark gray limestones that are generally thinly bedded. The Castle Reef Dolomite ranges in thickness from approximately 76 to 300 m and consists of thick, massive beds of medium to light gray dolostones [*Mudge*, 1972].

[9] Laramide deformation resulted in the formation of folds in the study area. Three folds were chosen for study because they are accessible and represent two different fold geometries (Figures 4b, 4c, and 4d). The Clary Coulee fold has a fault propagation fold geometry with one steeply dipping (78° to 93°E) eastern limb and one shallowly dipping (26° to 29°W) western limb. The Clary Coulee fold has a 23° plunge to the south. Approximately 3 km to the east of the Clary Coulee fold, the Teton anticline (Figure 4b) is best described as having a fault bend fold geometry that formed because of force applied to the area in the form of stress related to a thrust fault that did not make it to the surface. The Teton anticline has a 5° plunge to the south. Approximately 50 km to the northwest, the Swift Dam fold exhibits a similar fold structure as the Clary Coulee fold. The Swift Dam fold (Figures 4c and 4d) has a shallow western limb with dips ranging from 11° to 14°W and a steep eastern limb with dips ranging from 26° to 78°E. The Swift Dam fold plunges 10° to the northwest.

[10] Previous paleomagnetic studies on the Mississippian Madison Group have been conducted in different parts of the North American Cordillera. A study conducted in the Mesozoic units in the disturbed belt east of the study area found a pretilting to early syntilting magnetization interpreted to reside in magnetite [*Gill et al.*, 2002]. In the Canadian Cordillera, *Enkin et al.* [2000] found a pretilting–early syntilting CRM that is normal polarity in the Front Ranges and reverse polarity in the Inner Foothills to the east. *Beske-Diehl and Shive* [1978] found Late Cretaceous and Late Paleozoic remagnetizations in the Madison Group at Sheep Mountain, Wyoming. A paleomagnetic study to the south of the study area near the Helena salient of the Late Cretaceous Two Medicine Formation indicates an 11.7 ± 11.4° counterclockwise rotation of the thrust sheets [*Jolly and Sheriff*, 1992].

[11] The Madison Group has also been studied extensively for its oil and gas potential [e.g., *Dolson et al.*, 1993]. Dolomite distribution and diagenesis have been found to be important factors controlling porosity and consequently reservoir quality in the Madison Group [*Nichols*, 1980; *Pasternack*, 1988]. Hydrocarbons are interpreted to have migrated vertically through fractures in the Madison Group and laterally from west to east through the upper part of the Madison Group below Jurassic shales which served as seals [*Dolson et al.*, 1993].

3. Methodology

[12] Samples for paleomagnetic, rock magnetic, and geochemical analyses were collected in limestones and dolostones of the Madison Group, west of the easternmost limit of the disturbed belt along several east-west trending canyons incised by rivers (Figures 1 and 2). Cores were collected from 21 sites (approximately eight samples each) across seven thrust sheets in the Sun River Canyon from the Diversion thrust in the east to the Big George thrust in the west. Along the North and South Forks of the Teton River, cores were collected from 15 sites across five thrust sheets. Along the North Fork of the Teton River, cores were collected from 16 sites on the Clary Coulee fold. Cores were taken from 26 sites on the Teton anticline ~3 km to the east of the Clary Coulee fold. To the north at the Swift Reservoir, cores were collected from nine sites on the fold.

[13] A gasoline-powered portable drill was used to collect the cores which were oriented with an inclinometer and a Brunton compass. Cores were marked and cut to standard lengths (2.2 cm). The natural remanent magnetizations (NRMs) of the specimens were acquired using a 2G Enterprises cryogenic magnetometer (Model 755-1.65) with DC squids. In a magnetically shielded room, cores were subjected to thermal demagnetization for 1 hour at 22 increasing temperature steps between 100° and 600°C: NRM, 100, 150, 200, 250, 275, and 300–600 by 20°C steps. At higher

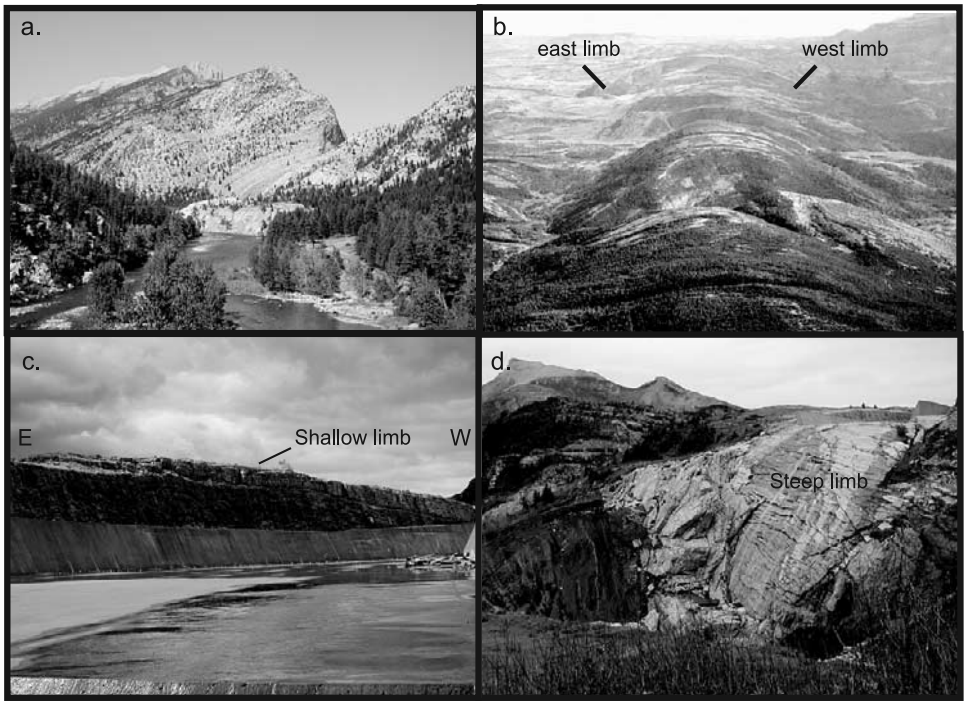

Figure 4. Photographs of (a) Sawtooth thrust sheet taken from the French thrust in the Sun River Canyon facing east, (b) Teton anticline looking south, (c) Swift Dam fold showing the shallow limb, and (d) Swift Dam fold showing the steep limb.

temperatures the magnetization was unstable. Thermal demagnetization was accomplished using an ASC Scientific Thermal Specimen Demagnetizer (Model TD-48 SC). Representative specimens were subjected to alternating field (AF) demagnetization in a 2G AF demagnetizer.

[14] Demagnetization data were plotted on *Zijderveld* [1967] diagrams using the Super-IAPD 99 software program. Principal component analysis [*Kirschvink*, 1980] was applied to determine the magnetic components in each specimen. The mean angular deviations (MADs) were $<10°$ except for specimens from the Clary Coulee and Swift Dam folds which tended to be between 10° and 15°. Site means were computed using *Fisher* [1953] statistics. Tilt tests were performed using the PMGSC [*Enkin*, 2004] version 4.2 software program. A filter with an α_{95} (cone of 95% confidence) of less than 20° was applied to the site means for the tilt tests. Tilt test results were used to obtain a pole position and compared to the North American apparent polar wander path (APWP) [*Besse and Courtillot*, 2002].

[15] Three tilt tests were performed on the demagnetization data. The direction-correction (DC) tilt test [*Enkin*, 2003] was used to determine optimal untilting statistics. For comparison, we also performed the *Watson and Enkin* [1993] k parameter tilt test, and partial untilting of individual sites was conducted using optimal differential untilting (ODU)/small circle analysis [*McCelland-Brown*, 1983; *Shipunov*, 1997; *Waldhöer and Appel*, 2006] using the PMSTAT [*Enkin*, 1997] version 4.1 software program.

[16] Low-temperature demagnetization [*Dunlop and Argyle*, 1991] was initially conducted on 146 representative specimens to investigate the possibility that a present-day viscous remanent magnetization (VRM) residing in multidomain magnetite overlaps the characteristic remanent magnetization (ChRM). The specimens were submerged in liquid nitrogen and subjected to temperatures below $-196°C$ for a period of 20–30 min. Placed in a shield, the specimens were allowed to warm to room temperature before remeasuring the NRM and thermally demagnetizing under normal procedures.

[17] Rock magnetic data were obtained through AF demagnetization, isothermal remanent magnetization (IRM) acquisi-

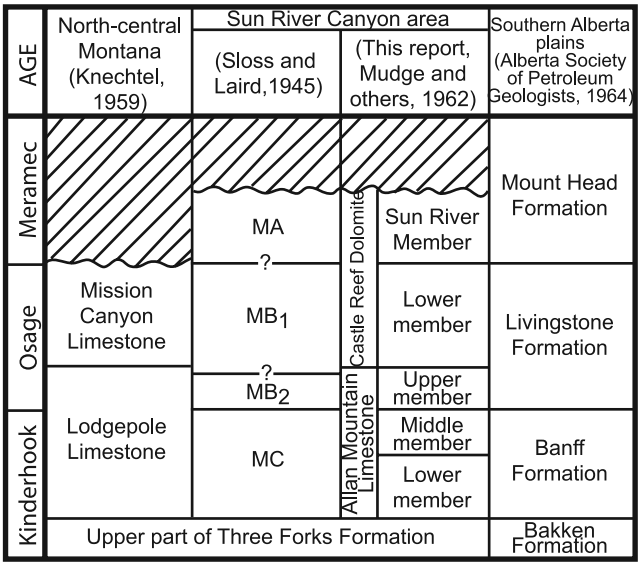

Figure 5. Mississippian stratigraphic column of the units in the study area [*Mudge*, 1972]. In this study, the Allan Mountain limestone and Castle Reef dolomite are the sampled lithologies.

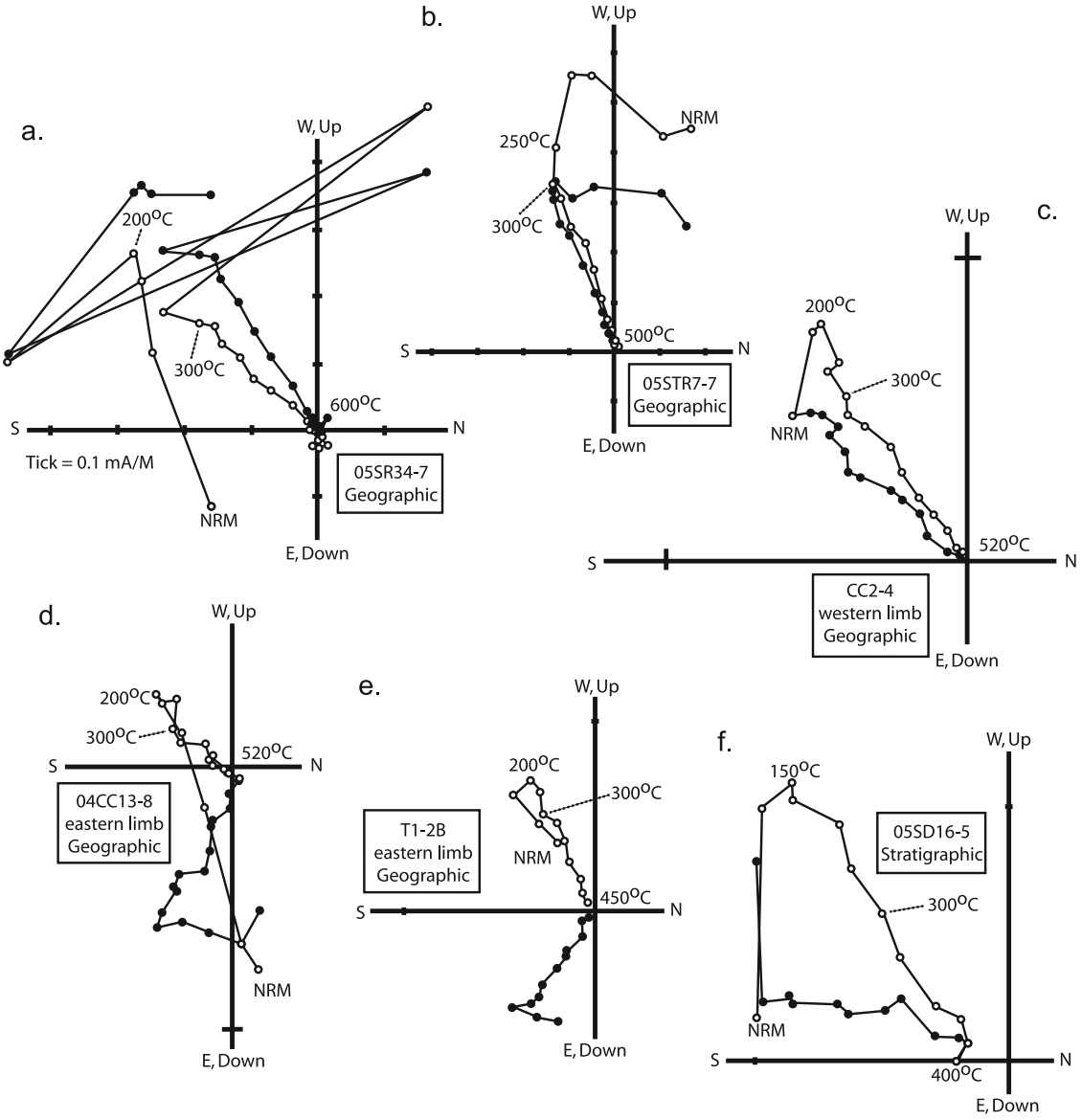

Figure 6. Representative Zijderveld diagrams from (a) the thrust sheets in the Sun River Canyon (VRM: 0–200°C; ChRM: 200–500°C), (b) the thrust sheets along the South Fork of the Teton River (VRM: 0–250°C; ChRM: 250–500°C), (c) the western limb of the Clary Coulee fold (VRM: 0–200°C; ChRM: 200–520°C), (d) the eastern limb of the Clary Coulee fold (VRM: 0–200°C; ChRM: 200–460°C), (e) the eastern limb of the Teton anticline (VRM: 0–200°C; ChRM: 200–450°C), and (f) the Swift Dam fold (VRM: 0–150°C; ChRM: 150–400°C). Open circles represent inclinations (vertical component), and solid circles represent declinations (horizontal component). Noise around the origin was removed from the projections except from Figure 6a. Tick marks are at 0.1 mA/M.

tion, and thermal decay. Thirty-one representative specimens underwent AF demagnetization from 0 to 120 mT using a 2G Automated Degaussing System. The specimens were subjected to IRM acquisition up to 2500 mT using an ASC Scientific Impulse Magnetizer (Model IM-10-30). The specimens underwent AF demagnetization for a second time from 0 to 120 mT. An IRM was imparted to the specimens in three perpendicular directions: 120, 500, and 2500 mT [*Lowrie*, 1990]. Last, the specimens were thermally demagnetized from which triaxial decay curves were determined.

[18] Petrographic analysis using transmitted and reflected light was used to identify magnetic phases and other diagenetic features. Strontium isotope analysis was performed at the University of Texas (Austin) in two batches (years 2004 and 2005) according to the methods described by *Gao et al.* [1992] on 15 limestone and dolostone samples from the study area. The NIST SRM 987 standard mean value was 0.710266 ± 0.000008 (2004 samples) and 0.710260 ± 0.000008 (2005 samples) (2σ = 0.000015, n = 41) and was used throughout the procedure. The strontium values were normalized relative to the National Bureau of Standards' NBS 987 = 0.71014. The $^{87}Sr/^{86}Sr$ values were then plotted and compared to the coeval seawater values for

Table 1. Site-Mean Statistics Used for Fold Test[a]

					Geographic				Stratigraphic				
Site	Latitude/Longitude	Strike/Dip, deg	Lithology	N/N_o	D, deg	I, deg	k	α_{95}, deg	D, deg	I, deg	k	α_{95}, deg	ODU, %
Sun River Canyon Thrust Sheets													
04SR7	47.62°N/112.71°W	200/24W	FP	7/8	206.7	−66.6	119.2	5.6	160.1	−59.0	119.2	5.6	22.7
04SR8	47.62°N/112.71°W	185/30W	FP	7/7	211.5	−66.4	154.9	4.9	144.8	−62.0	154.9	4.9	5.4
04SR9	47.62°N/112.73°W	185/46W	FP	8/8	253.4	−36.7	636.3	2.2	201.4	−71.1	636.3	2.2	99.0
04SR10	47.62°N/112.73°W	185/40W	FP	6/8	188.0	−57.6	12.4	19.8	140.7	−41.7	12.4	19.8	0.1
04SR11	47.61°N/112.74°W	177/52W	DW	7/9	249.0	−40.8	10.7	19.4	160.1	−75.9	10.7	19.4	77.2
04SR12	47.61°N/112.74°W	177/52W	FG	3/7	230.8	−34.3	62.6	15.7	173.1	−60.7	62.6	15.7	80.7
04SR13	47.61°N/112.75°W	169/55W	FG	7/8	217.6	−57.8	766.8	2.2	116.3	−54.4	766.8	2.2	28.7
04SR14	47.61°N/112.75°W	169/55W	FP	4/8	237.6	−50.5	136.7	7.9	117.5	−68.1	136.7	7.9	50.0
04/05SR15	47.61°N/112.76°W	176/66W	FP	12/16	238.5	−41.1	41.3	6.8	132.6	−61.4	41.3	6.8	57.1
04SR19[b]	47.60°N/112.79°W	182/79W	CD	6/8	246.9	−20.6	10.9	21.2	157.2	−64.0	10.9	21.2	-
04SR21	47.60°N/112.78°W	165/74W	FP	6/6	239.6	−18.1	105.5	6.6	154.7	−75.1	105.5	6.6	79.8
05SR31	47.60°N/112.78°W	158/67W	FP	7/8	242.8	−25.9	15.6	15.7	125.2	−84.5	15.6	15.7	74.1
05SR34	47.61°N/112.76°W	164/64W	FP	8/8	234.9	−35.0	235.1	3.6	130.8	−71.3	235.1	3.6	64.8
05SR35	47.61°N/112.75°W	176/61W	FP	8/8	222.9	−46.0	54.1	7.6	137.0	−52.4	54.1	7.6	44.6
05SR36	47.61°N/112.74°W	175/55W	CD	8/8	260.1	−60.2	159.3	4.4	90.7	−64.6	159.3	4.4	36.8
05SR37	47.61°N/112.74°W	172/51W	DM	8/8	231.3	−55.9	71.7	6.6	122.1	−63.6	71.7	6.6	38.3
05SR38[b]	47.62°N/112.73°W	186/42W	DW	3/8	219.2	−75.8	30.8	22.6	116.5	−54.1	30.8	22.6	-
North and South Forks of the Teton River Thrusts													
04DJ1	47.89°N/112.72°W	160/45W	CD	6/7	231.6	−32.5	87.3	7.2	195.0	−71.1	87.3	7.2	82.6
LP1	47.89°N/112.72°W	169/45W	FP	5/5	233.6	−43.6	23.3	16.2	164.5	−71.8	23.3	16.2	58.3
05LP2	47.89°N/112.72°W	173/52W	IG	8/8	227.5	−49.3	399.9	2.8	137.5	−62.2	399.9	2.8	38.7
05LP3	47.88°N/112.70°W	163/22W	FP	8/8	214.2	−59.4	91.1	5.8	171.0	−71.2	91.1	5.8	32.2
05LP4	47.88°N/112.69°W	161/22W	FP	8/8	175.4	−71.3	60.6	7.2	118.8	−65.3	60.6	7.2	0.0
04STR1	47.87°N/112.71°W	171/37W	FW	8/8	227.1	−45.7	385.6	2.8	175.8	−67.0	385.6	2.8	58.5
04STR2	47.87°N/112.72°W	171/51W	CD	8/8	235.7	−48.3	305.4	3.2	135.7	−69.6	305.4	3.2	43.8
04STR3	47.87°N/112.73°W	175/66W	FG	8/8	228.0	−29.3	297.8	3.2	157.6	−56.6	297.8	3.2	61.6
04STR4[b]	47.87°N/112.74°W	171/63W	CG	7/9	198.1	−13.0	40.9	9.6	171.1	−29.9	40.9	9.6	-
04STR5	47.87°N/112.75°W	180/42W	FP	7/8	224.6	−39.2	418.9	3.0	178.1	−56.5	418.9	3.0	66.7
05STR6	47.87°N/112.71°W	165/40W	FW	8/8	228.6	−56.2	112.7	5.2	133.3	−73.1	112.7	5.2	34.0
05STR7	47.87°N/112.72°W	175/50W	CD	8/8	250.0	−49.1	147.2	4.6	129.5	−76.0	147.2	4.6	51.5
05STR8	47.87°N/112.73°W	168/67W	FG	7/7	241.0	−22.5	855.9	2.1	166.4	−74.3	855.9	2.1	75.3
05STR9	47.87°N/112.74°W	162/66W	FP	6/9	248.7	−15.9	101.5	6.7	230.3	−81.3	101.5	6.7	85.6
05STR10	47.87°N/112.75°W	175/27W	FP	8/8	234.9	−57.3	53.8	7.6	182.3	−74.1	53.8	7.6	51.4
Teton Anticline: Eastern Limb													
T1	47.89°N/112.65°W	11.5/27E	CD	7/8	126.1	−40.7	39.9	9.7	146.4	−63.4	39.9	9.7	87.9
T2	47.89°N/112.65°W	1.5/29E	CD	7/9	112.1	−48.0	46.7	8.9	142.7	−72.5	46.7	8.9	55.1
T3	47.89°N/112.66°W	2.5/30E	FP	7/7	122.6	−45.0	64.0	7.6	156.0	−66.7	64.0	7.6	58.9
T4	47.89°N/112.66°W	3.5/29E	DFP	7/13	108.6	−40.6	60.5	7.8	124.7	−67.6	60.5	7.8	84.1
T5	47.89°N/112.66°W	355.5/23E	FP	8/8	124.4	−45.1	224.8	3.7	148.2	−60.1	224.8	3.7	79.5
T6	47.89°N/112.66°W	0.5/27E	DFG	7/13	114.6	−32.4	58.8	7.9	128.4	−55.8	58.8	7.9	99.9
T7	47.89°N/112.66°W	356.5/26E	DFG	5/9	119.3	−33.0	27.2	14.9	135.5	−53.0	27.2	14.9	99.9
T8	47.89°N/112.66°W	349.5/28E	DFG	11/11	118.7	−35.7	82.5	5.1	140.8	−54.2	82.5	5.1	97.0
T9	47.89°N/112.66°W	345.5/22E	FP	8/9	116.8	−43.9	68.6	6.7	138.6	−57.7	68.6	6.7	75.1
T10	47.89°N/112.66°W	334.5/18E	FP	7/7	126.6	−50.5	131.6	5.3	150.0	−55.7	131.6	5.3	36.8
T27	47.87°N/112.65°W	357.5/31E	DFP	9/9	101.9	−50.2	355.0	2.7	137.0	−77.9	355.0	2.7	62.4
Teton Anticline: Western Limb													
T11[b]	47.88°N/112.66°W	146.5/12W	CD	2/5	140.9	−36.4	5.6	150.4	132.5	−34.3	5.6	150.4	-
T12	47.89°N/112.66°W	150.5/10W	FG	4/4	166.4	−56.8	29.3	17.3	150.7	−58.2	29.3	17.3	0.9
T13	47.88°N/112.66°W	137.5/18W	DFP	7/10	168.2	−65.0	86.3	6.5	125.9	−68.2	86.3	6.5	8.0
T14	47.88°N/112.67°W	143.5/25W	DFP	9/10	166.1	−56.0	41.3	8.1	126.8	−57.4	41.3	8.1	36.5
T15	47.88°N/112.67°W	137.5/27W	DFP	7/7	186.1	−58.8	50.8	8.6	130.4	−69.8	50.8	8.6	53.5
T16[b]	47.88°N/112.67°W	155.5/23W	DFP	1/7	186.4	−51.3	-	-	154.5	−57.5	-	-	-
T17	47.88°N/112.67°W	154.5/21W	DFW	7/10	198.4	−67.4	84.6	6.6	138.0	−73.2	84.6	6.6	58.4
T18	47.89°N/112.66°W	160.5/14W	CD	4/8	191.6	−82.8	29.3	17.3	101.6	−78.0	29.3	17.3	1.7
T19[b]	47.89°N/112.66°W	165.5/16W	CD	3/6	158.5	−61.0	25.0	25.2	133.8	−55.5	25.0	25.2	-
T21	47.89°N/112.66°W	170.5/11W	CD	8/9	144.3	−65.2	72.2	6.6	127.2	−58.8	72.2	6.6	26.6
T22[b]	47.89°N/112.66°W	170.5/11W	CD	3/12	106.0	−60.3	17.5	30.4	98.6	−50.6	17.5	30.4	-
T23	47.89°N/112.66°W	160.5/09W	CD	7/9	193.6	−63.8	84.2	6.6	175.3	−67.5	84.2	6.6	82.7
T24	47.89°N/112.67°W	160.5/10W	CD	6/6	180.3	−58.2	97.6	6.8	163.8	−60.2	97.6	6.8	86.6
T25	47.87°N/112.66°W	135.5/13W	DFP	6/7	142.2	−70.8	96.0	6.9	110.2	−69.1	96.0	6.9	0.1
Clary Coulee Fold													
04CC1	47.89°N/112.71°W	133/28W	CD	4/7	222.5	−42.3	23.4	19.4	287.9	−76.9	23.4	19.4	62.4
04CC2	47.89°N/112.71°W	160/29W	CD	5/9	211.6	−44.8	126.7	6.8	156.5	−81.5	126.7	6.8	42.8
CC4	47.89°N/112.71°W	135/27W	DP	3/6	207.0	−46.6	102.6	12.2	331.5	−88.5	102.6	12.2	22.8
CC5[b]	47.89°N/112.71°W	015/30E	DP	2/6	215.5	−22.2	716.6	9.3	-	-	716.6	9.3	-
04CC7	47.89°N/112.71°W	347/78E	CD	7/8	123.0	−42.1	20.6	13.6	235.8	−45.3	20.6	13.6	69.0
04CC8	47.89°N/112.71°W	351/90E	DP	4/8	105.9	−2.1	159.0	7.3	193.9	−65.5	159.0	7.3	100.0

Table 1. (continued)

Site	Latitude/Longitude	Strike/Dip, deg	Lithology	N/N_o	Geographic				Stratigraphic				ODU, %
					D, deg	I, deg	k	α_{95}, deg	D, deg	I, deg	k	α_{95}, deg	
04CC9	47.89°N/112.71°W	355/90E	CD	6/8	108.8	−19.2	47.7	9.8	237.4	−60.1	47.7	9.8	88.5
CC10	47.89°N/112.71°W	357/93E	DM	5/6	151.0	−26.8	30.0	14.2	229.1	−20.3	30.0	14.2	42.9
04CC11	47.89°N/112.71°W	127/26W	DP	5/8	213.8	−59.1	16.3	19.6	350.8	−73.8	16.3	19.6	0.0
04CC13	47.89°N/112.71°W	353/90E	DW	8/8	118.6	−13.0	50.1	7.9	215.3	−53.0	50.1	7.9	84.4
04CC14	47.89°N/112.71°W	357/93E	DW	8/8	128.4	−46.8	87.7	5.9	257.5	−27.6	87.7	5.9	49.0
04CC15	47.89°N/112.71°W	357/93E	DP	3/8	138.3	−45.4	68.8	15.0	251.9	−22.8	68.8	15.0	45.4
					Swift Dam Fold								
05SD13	48.17°N/112.87°W	302/26E	DM	6/8	171.8	−74.1	13.0	19.3	184.2	−44.6	13.0	19.3	13.1
05SD15	48.17°N/112.87°W	247/14W	DM	7/8	308.9	−73.8	45.4	9.1	184.2	−79.7	45.4	9.1	100.0
05SD16	48.16°N/112.87°W	192/12W	DM	8/8	175.3	−68.1	30.2	10.2	150.3	−52.6	30.2	10.2	12.5
05SD17	48.16°N/112.87°W	192/12W	DM	6/8	147.3	−75.4	88.2	7.2	131.8	−55.6	88.2	7.2	28.4
05SD18	48.16°N/112.87°W	195/11W	CD	7/8	229.2	−82.6	13.9	16.8	144.0	−71.0	13.9	16.8	100.0
05SD19	48.17°N/112.87°W	317/78E	CCS	5/8	96.7	−54.3	20.8	17.2	184.6	−30.9	20.8	17.2	44.5

[a] N/N_o is the number of specimens with direction versus the number of demagnetized specimens; D is declination; I is inclination; k is a measure of grouping, α_{95} is the 95% cone of confidence. Lithology: CD, crystalline dolomite; FP, fossiliferous limestone; DFP, dolomitzed fossilifersous packstone; DFG, dolomitized fossiliferous grainstone; FG, fossiliferous grainstone; DFW, dolomitzed fossiliferous wackestone; DW, dolomitized wackestone; IG, intraclastic grainstone; CG, crinoidal grainstone; DM, dolomitzed mudstone; DP, dolomitzed packstone; CCS, carbonate-cemented sandstone [*Dunham*, 1962]. ODU refers to the optimal differential untilting function of PMSTAT [*Enkin*, 2004]. The ODU values for the individual sites are shown, but the best grouping results are given in Table 2.

[b] Sites not included in the tilt tests.

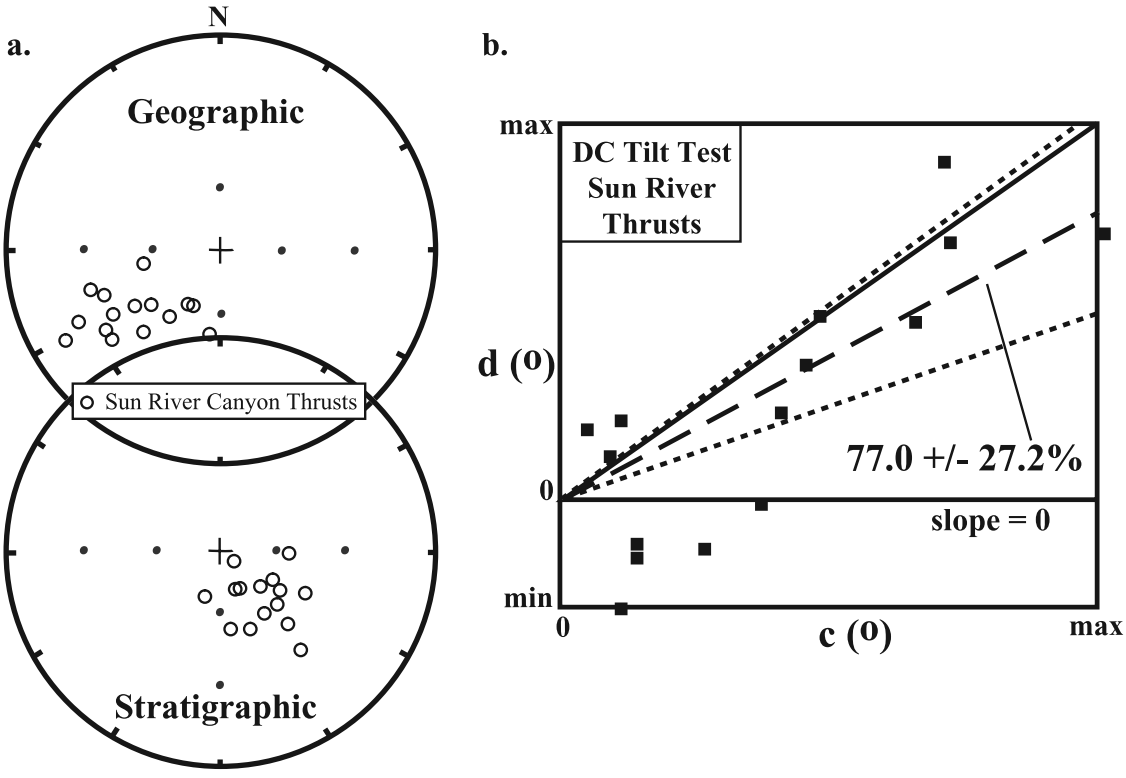

Figure 7. (a) Equal-area projection for the ChRM site means of the Sun River Canyon thrust sheets in geographic (0% untilting) and stratigraphic (100% untilting) coordinates. Open circles (all are negative inclinations) represent the site means from each sample location that was included in the direction-correction (DC) tilt test. The mean α_{95} of the Sun River Canyon sites is 8.6 (standard deviation of 6.0, n = 15). (b) DC tilt test results showing *d* versus *c,* where *c* is the angle between the geographic mean direction and the tilt-corrected site-mean direction that is back rotated by the angular relationship between the two directions and *d* is a projection of the arc between geographic site-mean directions and the geographic mean of means direction onto the arc used to calculate the *c* value [*Enkin*, 2003]. Optimal clustering is not significantly different than 100%, indicating a positive tilt test result. Dashed line indicates mean untilting percent; dotted lines indicate error bars.

Table 2. Tilt Test Results[a]

	N/N_o	D, deg	I, deg	k	α_{95}, deg	Percent Unfolding	Pole	dp, deg	dm, deg	β_{95}, deg
Sun River Canyon Thrust Sheets										
Direction-Correction	15/17	-	-	-	-	77.0 ± 27.2	-	-	-	-
Geographic	15/17	233.7	−47.4	19.0	9.0	0.0	44.7°N, 342.2°E	11.7	7.6	9.4
Stratigraphic	15/17	139.0	−66.4	29.7	7.1	100.0	63.0°N, 175.3°E	11.7	9.6	10.6
Best Grouping	15/17	171.2	−70.7	31.7	6.9	75.5 ± 11.6	80.8°N, 213.9°E	12.0	10.4	11.2
ODU	15/17	200.5	−69.4	109.8	3.7	-	75.9°N, 306.8°E	6.3	5.4	5.8
North and South Forks of the Teton River Thrusts										
Direction-Correction	14/15	-	-	-	-	95.7 ± 36.1	-	-	-	-
Geographic	14/15	231.9	−45.1	20.2	9.1	0.0	44.6°N, 346.1°E	11.5	7.3	9.2
Stratigraphic	14/15	159.4	−71.1	50.5	5.6	100.0	75.2°N, 196.3°E	9.8	8.5	9.1
Best Grouping	14/15	167.6	−71.4	50.8	5.6	93.6 ± 7.2	78.9°N, 208.9°E	9.8	8.6	9.2
ODU	14/15	208.6	−66.1	105.3	3.9	-	71.0°N, 324.9°E	6.4	5.2	5.8
Teton Anticline										
Direction-Correction	21/25	-	-	-	-	97.8 ± 15.3	-	-	-	-
Geographic	21/25	135.5	−56.3	14.2	8.7	0.0	55.9°N, 155.1°E	12.5	9.0	10.7
Stratigraphic	21/25	139.1	−64.8	62.5	4.1	100.0	62.6°N, 170.3°E	6.6	5.3	5.9
Best Grouping	21/25	138.9	−64.6	62.7	4.0	97.3 ± 6.5	62.4°N, 169.9°E	6.4	5.2	5.8
ODU	21/25	143.8	−63.5	53.0	4.4	-	65.1°N, 164.4°E	7.0	5.5	6.2
Clary Coulee Fold										
Direction-Correction	11/12	-	-	-	-	60.8 ± 21.7	-	-	-	-
Geographic	11/12	130.7	−62.1	4.5	24.3	0.0	55.8°N, 168.4°E	37.8	29.3	33.3
Stratigraphic	11/12	239.6	−60.4	7.5	17.9	100.0	48.1°N, 323.3°E	27.2	20.7	23.7
Best Grouping	11/12	208.4	−74.0	15.5	12.0	60.9 ± 4.5	69.6°N, 289.9°E	21.7	19.5	20.6
ODU	11/12	219.4	−68.8	60.3	5.9	-	64.7°N, 312.7°E	10.0	8.5	9.2
Swift Dam Fold										
Direction-Correction	6/6	-	-	-	-	45.5 ± 34.2	-	-	-	-
Geographic	6/6	145.3	−70.4	16.8	16.8	0.0	67.7°N, 186.7°E	29.1	25.1	27.0
Stratigraphic	6/6	165.0	−57.7	13.8	18.7	100.0	75.3°N, 120.4°E	27.4	20.1	23.5
Best Grouping	6/6	157.1	−65.9	29.6	12.5	43.9 ± 17.1	74.8°N, 165.6°E	20.4	16.7	18.4
ODU	6/6	154.6	−65.3	55.5	9.1	-	73.0°N, 163.9°E	14.7	11.9	13.3

[a] N/N_o is the number of sites used in the analysis versus the number of sites listed in Table 1; D is declination; I is inclination; k is a measure of grouping, a_{95} is the 95% cone of confidence. Percent untilting and confidence interval from direction-correction tilt test [*Enkin*, 2003] and *Watson and Enkin* [1993] fold test; best grouping from *Watson and Enkin* [1993]; dp/dm is the semiminor and semimajor axis, respectively, of the 95% error ellipse; B95 $(dp \times dm)^{1/2}$ is the oval of 95% confidence about the pole.

Mississippian age carbonates (Osagean to Meramecian) [*Denison et al.*, 1994; *McArthur et al.*, 2001].

4. Results and Interpretations

4.1. Paleomagnetism

[19] Thermal demagnetization removed a component interpreted as a present-day VRM at low temperatures (<200–300°C) and a ChRM between ~300°C and ~540°C in most specimens from the Madison Group (Figures 6a, 6b, 6c, 6d, 6e, and 6f). The maximum unblocking temperature ranges are similar for all locations (440–540°C), except for the Swift Dam fold which is lower (440–480°C). The ChRM (geographic coordinates) has southwesterly to southeasterly declinations and shallow to moderately steep up inclinations from the thrust sheets and folds. The ChRM is also removed by AF demagnetization, but the demagnetization trajectories are commonly curved and thermal treatment was the preferred demagnetization technique.

[20] Analysis of the 146 specimens that were subjected to low-temperature demagnetization shows a decrease in NRM intensities ranging from ~5 to 55%. Thermal demagnetization of the specimens shows no difference in component directions when compared to the specimens that were not subjected to low-temperature demagnetization. These results suggest that some multidomain magnetite is present, but it does not contribute to the ChRM.

4.1.1. Thrusts

4.1.1.1. Sun River Canyon

[21] Most sites from this area that are included in the tilt tests exhibit high (more than six or eight) numbers of specimens used in statistics compared to specimens analyzed (Table 1). The 95% cone of confidence (α_{95}) are <10° in 11 sites, <20° in 4 sites, and >20° in two sites (not included in the tilt tests). The measure of grouping for each site, represented by the *k* parameter, ranges in value from 10.7 to 766.8.

[22] The site means display a better grouping in stratigraphic coordinates than in geographic coordinates, suggesting a pretilting ChRM (Figure 7a).The DC tilt test results for the thrust sheets in the Sun River Canyon indicate optimal untilting at 77.0 ± 27.2% (Figure 7b and Table 2). Although not a true fold test, the tilt test is positive; this indicates a pretilting acquisition ($D = 139.0°$, $I = -66.4°$; $\alpha_{95} = 7.1°$, $k = 29.7$, 100% untilting) in which the DC slope is like 100% and unlike 0%. The Watson and Enkin tilt test results indicate a best grouping at 75.5 ± 11.6% untilting (Table 2), which suggests the ChRM was acquired during an early stage of the thrusting event. The *Watson and Enkin* [1993] test underestimates the error and the DC tilt test is considered to provide a better estimate of error [*Enkin*, 2003]. The individual site

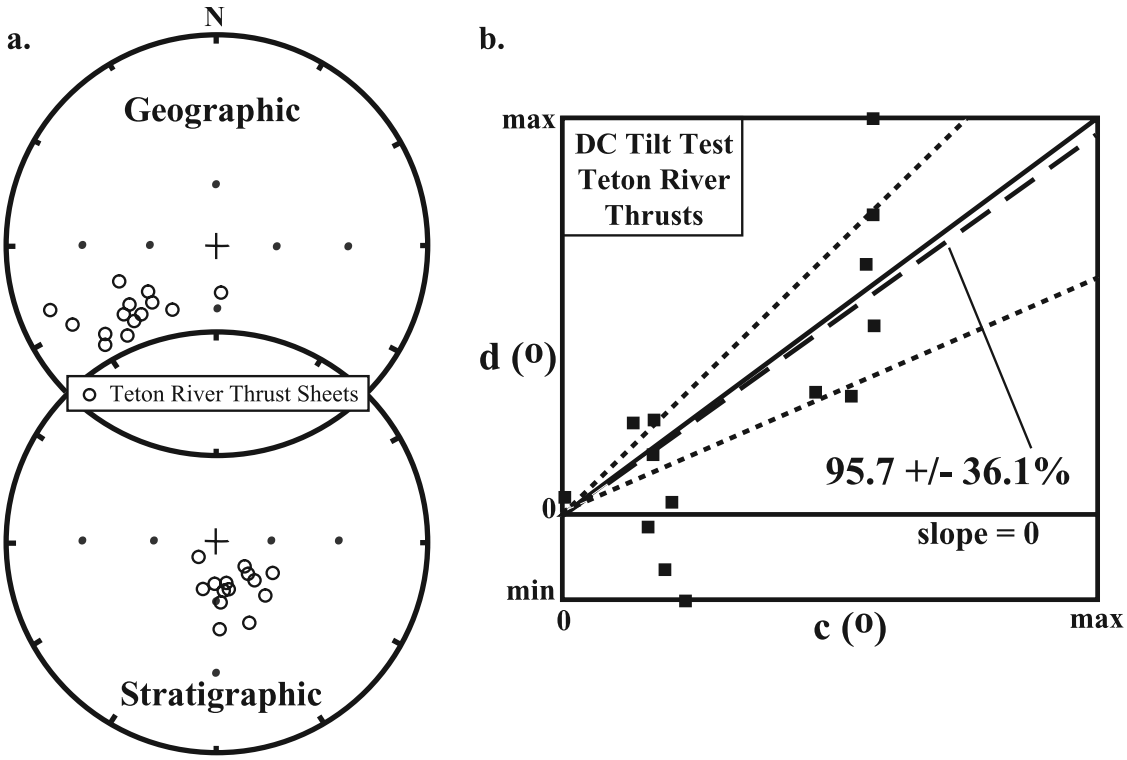

Figure 8. (a) Equal-area projection for the ChRM site means of the Teton River thrust sheets in geographic (0% untilting) and stratigraphic (100% untilting) coordinates. The mean α_{95} of the Teton River sites is 5.5 (standard deviation of 3.6, n = 14). (b) DC tilt test results. Optimal clustering is not significantly different than 100%, indicating a positive tilt test result. Conventions are the same as in Figure 7.

partial untilting values in the ODU analysis give a wide range of values (0.1 to 99.0%, Table 1), and the mean direction (Table 2) is different from the tilt test results. If there is a wide variability in ODU untilting percentages, then one should question whether the test is valid. If the orientation of the beds is parallel or nearly so, as they are in the study area, the small circle paths never cross, which limits the value of the test [e.g., *Waldhöer and Appel*, 2006].

4.1.1.2. North and South Forks of the Teton River

[23] All sites included in the tilt tests but one have high N/N_o values and low (<10°) α_{95} values (Table 1). The k parameter is good to excellent for all sites and ranges from 23.3 to 855.9. The site means display a better grouping in stratigraphic coordinates than in geographic coordinates, suggesting a pretilting ChRM (Figure 8a). For the thrust sheets in the North and South Forks of the Teton River, the DC tilt test results indicate optimal untilting at 95.7 ± 36.1% (Figure 8b and Table 2). The tilt test is positive, which indicates a pretilting acquisition with D = 159.4°, I = −71.1° (α_{95} = 5.6°, k = 50.5, 100% untilting). The Watson and Enkin tilt test results indicate a best grouping at 93.6 ± 7.2% untilting (Table 2). The confidence interval overlaps 100% untilting suggesting a pretilting remagnetization in which the ChRM was acquired before the thrusting event. Similar untilting percentages were obtained from the Watson and Enkin and DC tilt tests. Individual site partial untilting during the ODU analysis gave a range of values from 0.0 to 85.6%. The mean direction (Table 2) is different from the tilt test results, perhaps because the small circle paths do not cross during untilting.

4.1.2. Folds

4.1.2.1. Teton Anticline

[24] Sites from this area that are included in the tilt tests exhibit high N/N_o values and low α_{95} values (Table 1). The k parameter ranges from 27.2 to 355.0. The site means display a better grouping in stratigraphic coordinates than in geographic coordinates, suggesting a pretilting ChRM (Figure 9a). The DC tilt test results for the Teton anticline indicate optimal untilting at 97.8 ± 15.3% (Figure 9b and Table 2). The tilt test is positive, which indicates a pretilting acquisition with D = 139.1°, I = −64.8° (α_{95} = 4.1°, k = 62.5, 100% untilting). The Watson and Enkin tilt test results indicate a best grouping at 97.3 ± 6.5% untilting (Table 2). The results also suggest a pretilting magnetization. The mean direction obtained using ODU analysis is declination (D) = 143.8°, inclination (I) = −63.5° (α_{95} = 4.4°, k = 53.0, Table 2). Individual site partial untilting (Table 1) gave a range of values from 0.1 to 99.9%, perhaps because the strikes are similar from both limbs.

[25] We sampled in and around two well developed stylolites (sites T8 and T9) to test for a connection between pressure solution and remagnetization. There were no differences in the NRM intensities or the ChRM directions compared to proximity to the stylolites. As a result, we find no evidence that pressure solution was a factor in remagnetization.

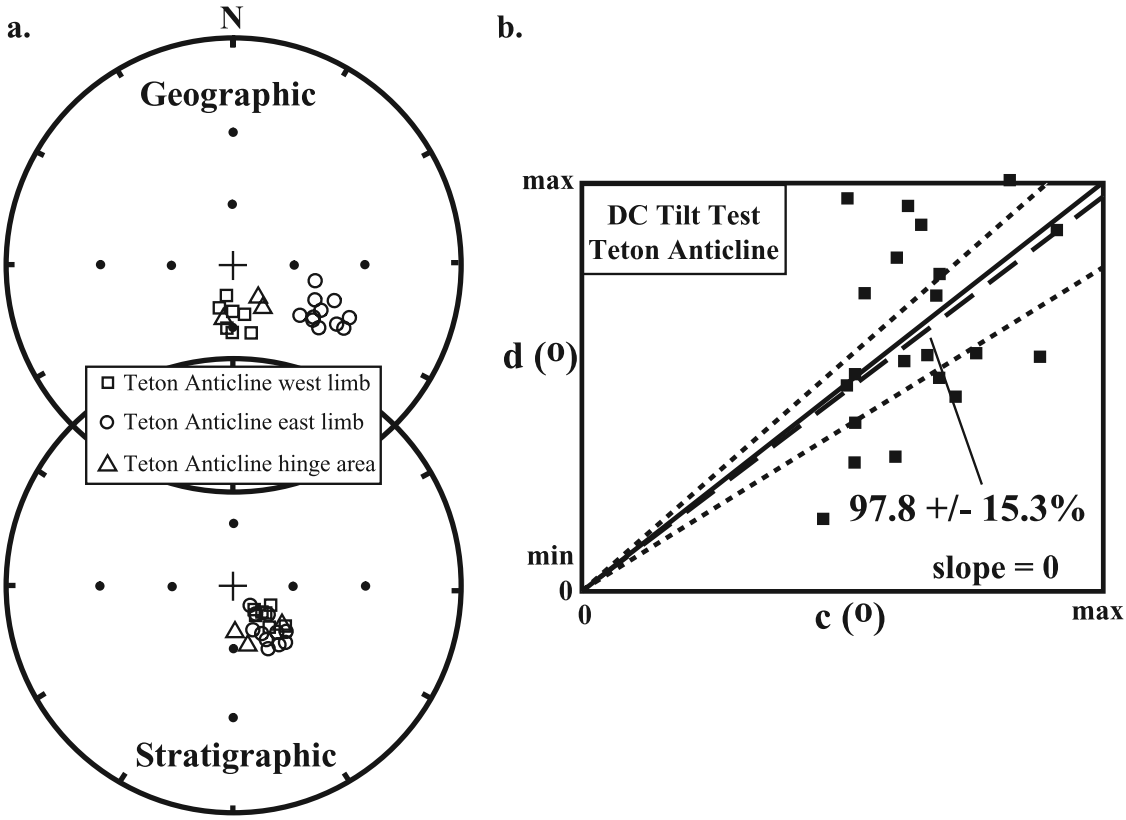

Figure 9. (a) Equal-area projection for the ChRM site means of the Teton anticline in geographic (0% untilting) and stratigraphic (100% untilting) coordinates. Circles represent the east limb, squares represent the west limb, and triangles represent the hinge area of the fold. The mean α_{95} of the Teton anticline sites is 8.2 (standard deviation of 3.9, n = 21). (b) DC tilt test results. Optimal clustering is not significantly different than 100%, indicating a positive tilt test result. Conventions are the same as in Figure 7.

4.1.2.2. Clary Coulee Fold

[26] The N/N_o for sites from this area (Table 1) that are included in the tilt tests range from low (3/8) to high (8/8). The α_{95} values for the 12 sites which contain the ChRM are <20°. The k parameter is good to excellent for all sites and ranges from 16.3 to 716.6. The site means from the two limbs appear to cross during untilting, suggesting a syntilting component (Figure 10a). The DC tilt test results for the Clary Coulee fold indicate optimal untilting at 60.8 ± 21.7% (Figure 10b and Table 2). The tilt test is indeterminate which indicates a syntilting acquisition or an incomplete separation of pretilting and posttilting components. The Watson and Enkin tilt test results (22° plunge correction) indicate a best grouping at 60.9 ± 4.5% untilting with D = 208.4°, I = −74.0° (α_{95} = 12.0°, k = 15.5, N/N_o = 11/12; Figure 10c and Table 2). The results suggest a syntilting remagnetization in which the ChRM was acquired during tilting. The mean direction obtained using ODU analysis is D = 219.4°, I = −68.8° (α_{95} = 5.9°, k = 60.3; Table 2). Individual site partial untilting gave a range of values from 0.0 to 100.0% (Table 1). Similar directional results were obtained from the different tilt tests.

4.1.2.3. Swift Dam Fold

[27] The N/N_o for sites from this area (Table 1) that are included in the tilt tests range from 5/8 to 8/8. The α_{95} values for all 6 sites that contain the ChRM are <20°. The k parameter ranges from 13.0 to 88.2. The site means from the two limbs appear to cross during untilting, suggesting a syntilting component (Figure 11a). The DC tilt test results for the Swift Dam fold indicate optimal untilting at 45.5 ± 34.2% (Figure 11b and Table 2). The tilt test is indeterminate, which suggests a syntilting acquisition. The Watson and Enkin tilt test results (10° plunge correction) indicate a best grouping at 43.9 ± 17.1% untilting with D = 157.1°, I = −65.9° (α_{95} = 12.5°, k = 29.6, N/N_o = 6/6; Table 2). The results suggest a syntilting remagnetization. The mean direction obtained using ODU analysis is D = 154.6°, I = −65.3° (α_{95} = 9.1°, k = 55.5; Table 2). Individual site partial untilting gave a range of values from 12.5 to 100% (Table 1). Similar directional results from the different tilt tests were obtained, and all suggest a syntilting remagnetization.

4.1.3. Paleopoles

[28] The poles for the three pretilting ChRMs lie close to or on the late Jurassic to early Tertiary part of the North American APWP (Figure 12). A mean pole for the three pretilting poles is 67.2°N, 177.9°E (A_{95} = 13.1°), which suggests remanence acquisition during the late Jurassic to Cretaceous. The Swift Dam fold pole (74.8°N, 165.6°E; Table 2) has a large margin of error and overlaps the Cretaceous and Tertiary part of the path, and the Clary Coulee pole (69.6°N, 289.9°E; Table 2) is off the path (Figure 12).

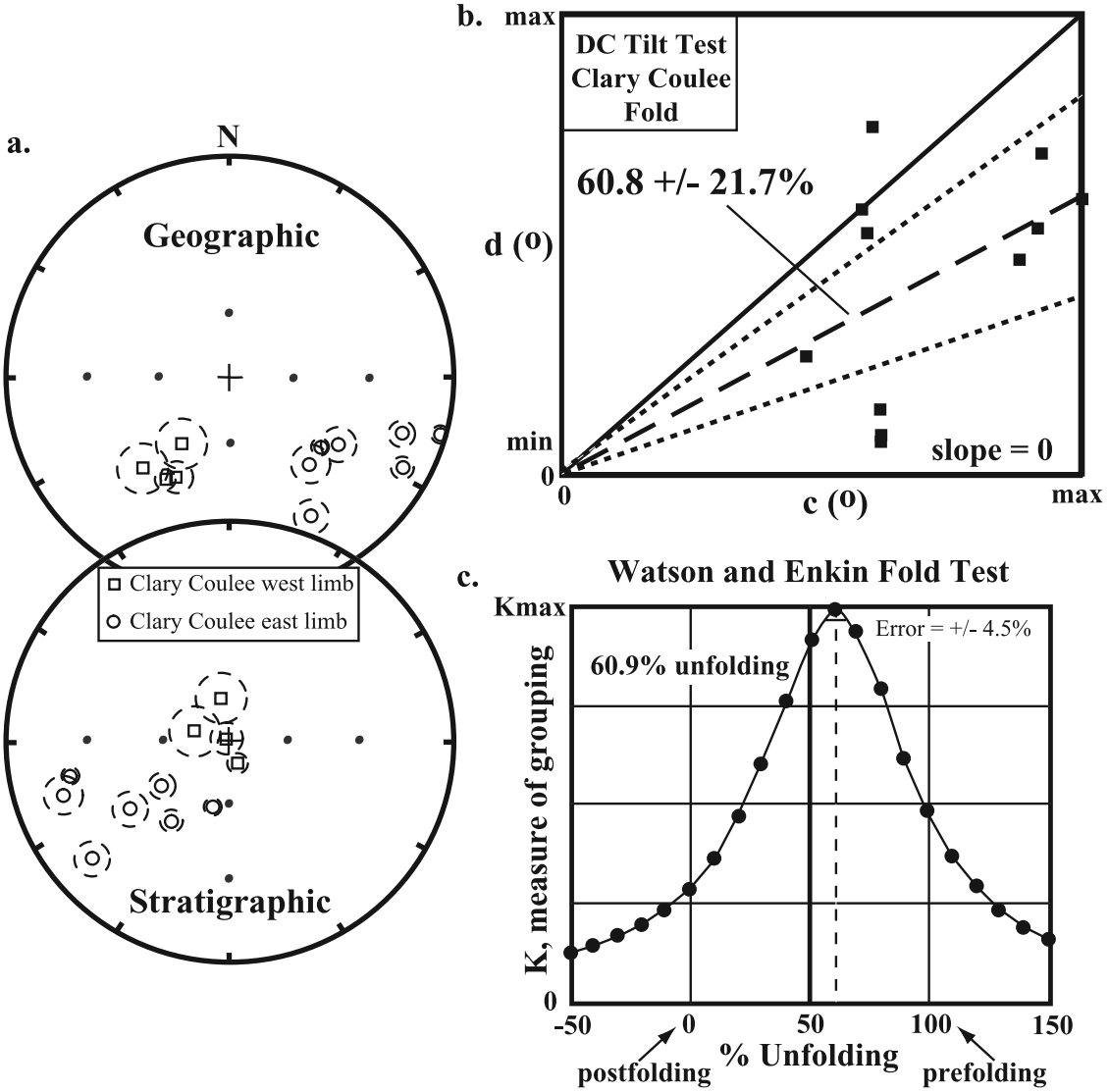

Figure 10. (a) Equal-area projection for the ChRM site means of the Clary Coulee fold in geographic (0% untilting) and stratigraphic (100% untilting) coordinates. Circles represent the east limb and squares represent the west limb on the fold. The dashed circles represent the α_{95} of the site means. (b) DC tilt test results. Optimal clustering indicates an indeterminate tilt test result in which there was a syntilting acquisition or an incomplete separation of pretilting and posttilting components. Conventions are the same as in Figure 7. (c) Watson and Enkin fold test showing the percent unfolding for the Clary Coulee fold with k (measure of grouping) on the y axis versus percent unfolding on the x axis. Dashed line represents the percent unfolding indicating a syntilting acquisition, which is not significantly different than the DC tilt test result. The error is also shown by the horizontal line on the graph.

4.1.4. Summary

[29] These results suggest that the ChRM in the thrust sheets and Teton anticline was acquired prior to deformation, whereas the ChRM in the Clary Coulee and Swift Dam folds is apparently coeval with Laramide deformation.

[30] Most specimens in sites that were not used in the statistical data analysis contain the ChRM, but the MAD angles were high (>15°), α_{95} was high (>20°), and/or the number of specimens (N) used in the analysis was low (<3). Some sites (four from Sun River Canyon, one from the Teton anticline, four from the Clary Coulee fold, and three from the Swift Dam fold) are not included in Table 1 because they do not contain the ChRM. The specimens in these sites exhibit weak magnetic intensities and/or are dominated by the present-day VRM.

4.2. Rock Magnetism

[31] Alternating field demagnetization results for a representative specimen (Figure 13a) show significant decay (~90%) of the NRM by 120 mT suggesting a low-coercivity phase dominates the NRM. Isothermal remanent magnetization (IRM) acquisition (Figure 13b) curves for specimens from the study area commonly reach saturation by about 300–500 mT, suggesting the presence of a low-coercivity phase. A slight rise above 500 mT suggests the presence of some higher coercivity mineral such as hema-

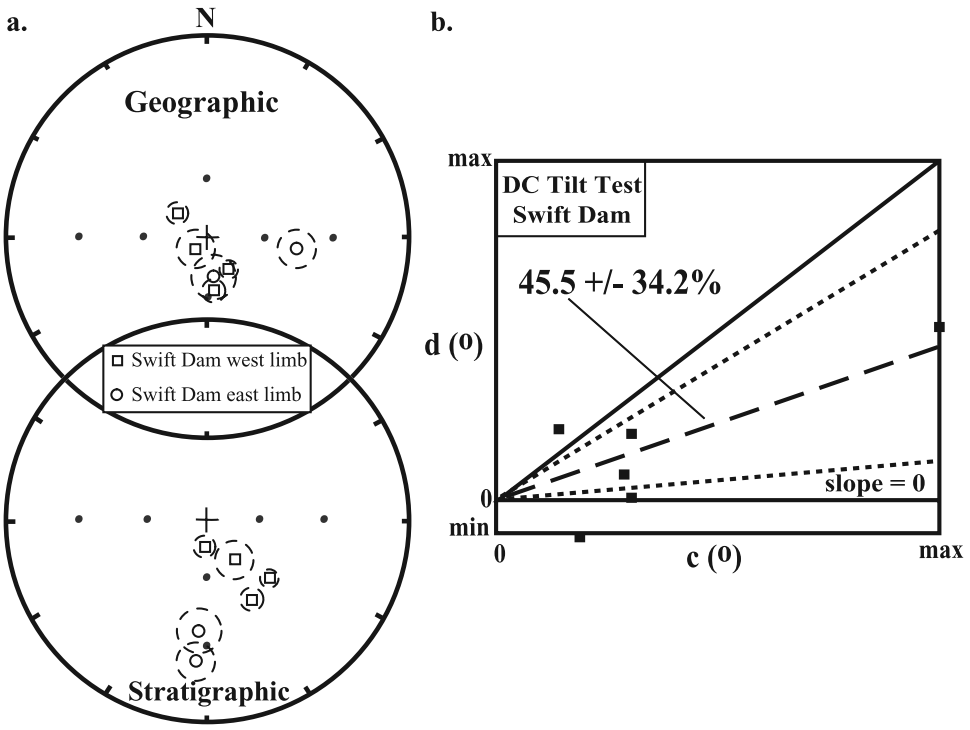

Figure 11. (a) Equal-area projection for the ChRM site means of the Swift Dam fold in geographic (0% untilting) and stratigraphic (100% untilting) coordinates. Circles represent the east limb and squares represent the west limb on the fold. The dashed circles represent the α_{95} of the site means. (b) DC tilt test results. Optimal clustering indicates an indeterminate tilt test result in which there was a syntilting acquisition or an incomplete separation of pretilting and posttilting components. Conventions are the same as in Figure 7.

tite. Alternating field decay of the IRM for most specimens removes most of the IRM. Thermal decay (Figure 13c) of a three-component IRM shows that the low-coercivity curve dominates and is removed by 580–600°C. This suggests the magnetization resides in magnetite. This result is common for limestone and some dolomite samples. No difference in rock magnetic behavior has been found between samples in sites with syntilting and pretilting results.

[32] Alternating field demagnetization for many dolomite and some limestone specimens shows less decay of the IRM (~55%) than the NRM (95%), suggesting a greater percentage of a high-coercivity phase than in most samples. Isothermal remanent magnetization curves for these specimens show an increase above 300 mT suggesting the presence of a high-coercivity mineral phase. In the triaxial thermal decay, the 500 and 2500 mT curves represent a more significant portion of the IRM, and they do not completely decay until above 650°C. This suggests that magnetite carries the bulk of the magnetization, and that a high-coercivity mineral such as hematite is also present. We compared the rock magnetic data with the directional data, and no relationships were evident. We see no evidence that hematite contributes significantly to the NRM.

4.3. Petrography

[33] Thin section and sample analysis using transmitted light indicates a predominance of fossiliferous packstones and grainstones in the thrust sheets according to the *Dunham* [1962] classification for carbonate rocks. The Teton anticline shows a predominance of dolomitized lithologies. The majority of samples from the Clary Coulee and Swift Dam folds are crystalline dolomite and/or dolomitized mudstone. Stylolites are present in ~20% of the samples with no obvious differences in abundance between the folds and the thrust sheets. Calcite veins are present in ~40% of the samples. Calcite veins appear to be most abundant in samples from the steep flank of the Clary Coulee fold. Specimens from both types of sample localities (thrusts and folds) exhibit magnetite (and occasionally hematite) replacing pyrite (Figure 14a). Some specimens from the two folds contain obvious hydrocarbons in vugs (Figures 14b, 14c, and 14d).

4.4. Geochemistry

[34] Strontium isotope analysis was used as an alteration indicator. The 15 representative specimens that were analyzed had elevated $^{87}Sr/^{86}Sr$ values with a mean value of 0.7088 ± 0.0006 (Figure 15) as compared to coeval seawater values for Mississippian age carbonates (0.7075 to 0.7080) [*McArthur et al.*, 2001]. This suggests that there was alteration by externally derived fluids. It is also interesting to note that dolomites have a higher mean (0.7093 ± 0.0003) than limestones (0.7084 ± 0.0006).

[35] Preliminary fluid inclusion microthermometry of primary and pseudosecondary two-phase brine inclusions in calcite veins from the Madison Group in the Clary Coulee fold and adjacent thrust sheets gives homogenization values of 108° to 170°C and salinities of 0 to 13 wt %

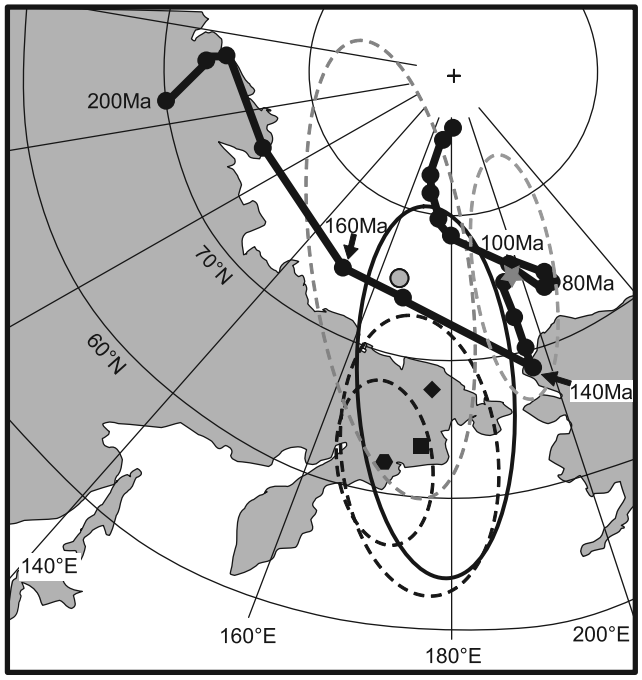

Figure 12. Close-up of the Mesozoic/Cenozoic portion of the North American apparent polar wander path with errors around the reference poles (modified from *Besse and Courtillot* [2002]). Poles from the study area are plotted with their ellipses of 95% confidence (dashed). The Swift Dam fold (circle), Sun River thrust sheets (square), Teton River thrust sheets (star), and Teton anticline (polygon) paleopoles plot on the late Jurassic to early Tertiary portion of the path. The mean pole for the latter three pretilting poles is 67.2°N, 177.9°E (diamond) and is plotted with the $A95$ (13.1°; solid line). The Clary Coulee fold is absent because its pole position lies on the other side of the globe from the path.

NaCl equivalent. On the basis of eutectic melting temperatures, these are NaCl-rich brines. Black liquid hydrocarbon inclusions and methane inclusions are commonly found associated with these brine inclusions. In addition, degraded hydrocarbon (bitumen) is commonly found as intercrystalline masses within the veins and in vugs. Inclusions in healed microfractures (secondary?) contain higher salinity $CaCl_2$-rich fluids with up to 23 wt % NaCl equivalent, and suggest that the Madison Group was infiltrated with fluids from deeper formations.

5. Discussion

[36] Paleomagnetic results demonstrate that a widespread ChRM is present in the Sawtooth Range that is pretilting in the thrust sheets and Teton anticline and syntilting in the Clary Coulee and Swift Dam folds. The magnetic characteristics within the study area are similar in that the maximum unblocking temperatures are similar, with exception of the Swift Dam fold in which the maximum unblocking temperature is slightly lower than the other areas. Magnetic intensities of the NRM are highly variable (~0.010–0.540 mA/m) and do not show any differences between the sampling areas. Rock magnetic results (from AF and thermal decay) do not reveal any differences in the data between the specimens from the two folds with syntilting results and the specimens with pretilting results (thrust sheets and Teton anticline). The thermal and AF demagnetization of the NRM, as well as the rock magnetic results, suggest that the ChRM resides in magnetite.

[37] The ChRM cannot be explained by a thermoviscous remanent magnetization, because burial temperatures of ~150°C, based on vitrinite reflectance [*Hoffman et al.*, 1976; *Hoffman and Hower*, 1979; *Becker*, 1988], are too low and inconsistent with the maximum unblocking temperatures greater than 500°C (average 502°C) based on the time-temperature unblocking curves of *Pullaiah et al.* [1975]. This suggests that the ChRM is a CRM.

5.1. Origin of the CRM

[38] A number of different chemical mechanisms for the origin of the CRM are possible. For example, a number of studies have explained CRMs as originating from alteration by externally derived fluids such as orogenic or basinal fluids [e.g., *McCabe and Elmore*, 1989; *Oliver*, 1992; *Elmore et al.*, 2001; *Blumstein et al.*, 2005]. Several studies have also proposed that hydrocarbons can cause remagnetization [*Elmore et al.*, 1987; *McCabe et al.*, 1987; *Elmore and Crawford*, 1990; *Elmore et al.*, 1993]. In addition, chemical remagnetizations can be caused by burial processes such as clay diagenesis [*Katz et al.*, 2000; *Moreau et al.*, 2005] and/or hydrocarbon maturation [e.g., *Banerjee et al.*, 1997; *Blumstein et al.*, 2004].

[39] The Madison Group rocks are not source rocks, so maturation of organic matter is not a viable remagnetization mechanism. Clay is not common in the Madison Group rocks, except in some intervals. In addition, it is not clear that there was enough burial heat to cause smectite to convert to illite. Burial depths of at least 2 km are needed for the conversion [e.g., *Chamley*, 1989]. Burial depths were too low in the Jurassic–early Cretaceous (<1 km, estimated from *Mudge* [1972]) although they were ~2400 m [*Mudge*, 1972] in the late Cretaceous. The pole positions do not provide enough resolution to resolve this issue. In any case, clay diagenesis is not a likely mechanism for the pervasive remagnetization.

[40] The elevated $^{87}Sr/^{86}Sr$ values and the fluid inclusion results suggest the Madison Group was altered by externally derived fluids. The veins and porous zones caused by dolomitization probably served as conduits for the fluids [e.g., *Dolson et al.*, 1993]. The presence of hydrocarbon and methane inclusions, as well as degraded hydrocarbons in vugs, suggest that hydrocarbons also migrated into the unit. Therefore, either hydrocarbons or fluids with radiogenic signatures could have caused the acquisition of the CRM. The remagnetization mechanism is interpreted to be an externally derived fluid and not a burial process.

5.2. Origin of Syntilting Remagnetizations

[41] The CRMs found in the study area all have the same characteristics and are probably caused by the same remagnetization event, yet the timing of remagnetization varies from pretilting in the thrust sheets and one fold to syntilting in two of the folds. Possible explanations for the difference in the tilt test results are discussed here. An overlapping of magnetic components resulting in contamination could

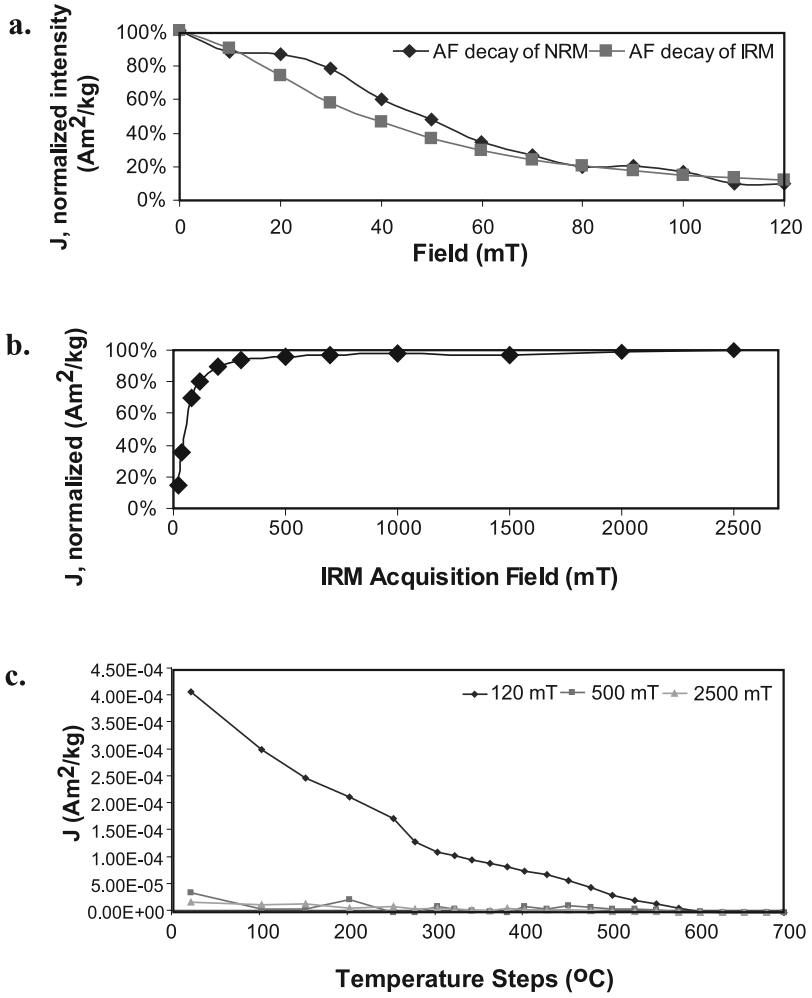

Figure 13. Rock magnetic results from a representative specimen (04SR14-8b). (a) AF demagnetization of the NRM and IRM, (b) IRM acquisition, and (c) triaxial thermal decay of the IRM.

explain the syntilting results on the two folds [e.g., *Elmore et al.*, 2006]. Although this is a possibility, it can be discounted because there is evidence for only one ancient secondary magnetic component in each specimen from the Madison Group. The CRMs and rock magnetic properties from the thrust sheets and the three folds are also similar, suggesting that there was only one remagnetization event.

[42] Another possible explanation for the differences in the tilt test results could be related to the difference in the fold types between the Teton anticline (fault bend fold geometry) and the Clary Coulee and Swift Dam folds (fault propagation fold geometry). Perhaps the deformation that caused the difference in fold type geometry caused variations in strain/stress (higher in Clary Coulee and Swift Dam folds), which may have modified an original pretilting CRM to a syntilting CRM. The fault propagation style folds have relatively straight back limbs and highly curved forelimbs. The bulk of the whole rock strain is probably accommodated in the forelimbs by brittle fracturing and pressure solution. The Teton anticline has a fault bend fold geometry. It is a straight-limbed fold, with most deformation in the curved hinge zone. The limbs were passively rotated and accommodate little folding strain.

[43] Several recent studies have speculated that strain and/or stress could have caused alteration of a pretilting magnetization into a syntilting configuration [*Lewchuk et al.*, 2003; *Elmore et al.*, 2006]. Other studies have shown that strain during folding may cause rotation of iron oxide grains which can change a pretilting into a syntilting remanence in sandstone units [e.g., *Stamatakos and Hirt*, 1994; *Stamatakos and Kodama*, 1991a, 1991b] but not in a carbonate unit such as the Allentown Dolomite [*Kodama*, 1988]. We did not unstrain the remanence [e.g., *Kodama*, 1988; *Borradaile*, 1997] when performing the tilt tests. It is not clear that the strain differences between the two fold types and the thrusts were high enough to cause rotations which could account for the tilt test results.

[44] Strain-enhanced chemical processes may also have caused dissolution of iron oxide grains in solution structures which resulted in precipitation of remanence carrying grains during folding [e.g., *Evans and Elmore*, 2006]. We found no magnetic differences in samples compared to proximity to the stylolites. Because of this, and the fact that solution structures are not common in the Madison Group in the sampling area, we do not think that a strain-enhanced process caused the pervasive remagnetization.

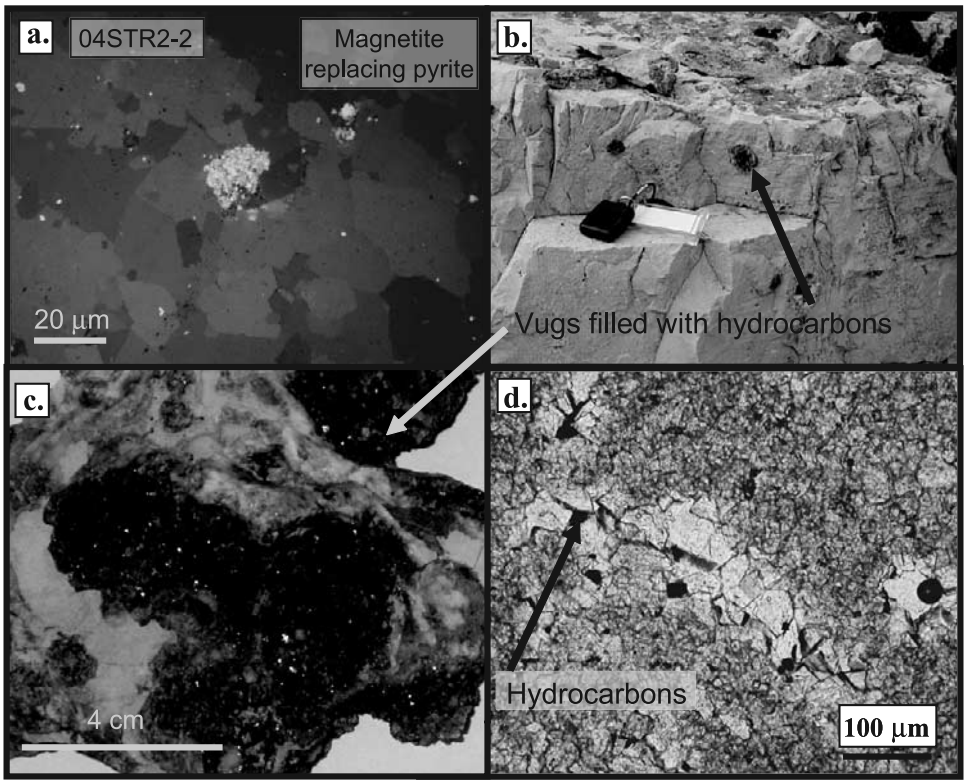

Figure 14. Thin section petrography and petrology. (a) Thin section of magnetite replacing pyrite from a representative specimen from Teton River thrust sheets in reflected light. Petrography and petrology of the Swift Dam fold: (b) study area photograph of vugs in the Mississippian Madison carbonates, (c) close-up of a vug filled with hydrocarbons, and (d) thin section of degraded hydrocarbons in vugs of dolomitized mudstone (transmitted light).

[45] A piezoremanent magnetization (PRM) [e.g., *Hudson et al.*, 1989; *Borradaile*, 1997] caused by higher stresses in the two fault propagation folds compared to the Teton anticline and the thrust sheets is also a possibility. This assumes that there were higher stresses in the former. Although this is a possibility, we have no direct evidence supporting this hypothesis.

[46] In addition to fold geometry, other factors such as the position of the sites on the fold and the kinematic history of the fold may influence the tilt test results. We should clarify that we are using fault bend and fault propagation folds as descriptive terms only and not genetically. We have no control over the kinematic development of the folds.

[47] In summary, a number of factors could account for the differences in the tilt test results. Additional studies are clearly needed to better understand the differences in the tilt test results between the different fold types in the Madison Group in the Sawtooth Range.

5.3. Remagnetization Trends

[48] Previous work in the North American Cordillera has shown that Cretaceous to early Tertiary CRMs are fairly common [e.g., *Enkin et al.*, 2000]. *Enkin et al.* [2000] found a pretilting to syntilting CRM in the Front Ranges and Inner Foothills of the Canadian Cordillera. The CRM has a normal polarity in the Front Ranges and a reverse polarity in the Inner Foothills. They conclude that the remagnetizations progressed from west to east in front of the Cordilleran deformation. The CRM was acquired over a long period of time, which explains the reversal. Finally, *Enkin et al.* [2000] suggest that the CRM was due to a pervasive diagenetic process related to orogenesis.

[49] A study conducted by *Stamatakos et al.* [1996] found a remagnetization trend across the thrust sheets in the North American Appalachians. The study found a posttilting CRM in the hinterland, a syntilting CRM in the central area, and a pretilting CRM in the foreland. *Cox et al.* [2005] also report that Devonian red beds contain a syntilting CRM in the Valley and Ridge province and a pretilting CRM in the foreland. Geochemical/fluid inclusion studies indicate that the rocks were exposed to mixed methane-saturated formational and meteoric fluids only, with no evidence that external hot orogenic fluids altered the rocks [*Cox et al.*, 2005]. They proposed a working model for CRM acquisition that involves methane reduction of previously formed iron phases and mobilization of iron followed by a return to oxidizing conditions and precipitation of new authigenic hematite as a result of the introduction of meteoric fluids just prior to and during uplift.

[50] In this regional study of the Sawtooth Range, a pretilting CRM was found in the thrust sheets, as well as in the Teton anticline and a syntilting CRM was found in the Clary Coulee and Swift Dam folds. In addition, *Gill et al.* [2002] report a pretilting magnetization in Mesozoic rocks in Subbelt I (Figure 1). These results from the disturbed belt do not provide evidence that the remagnetization progressed

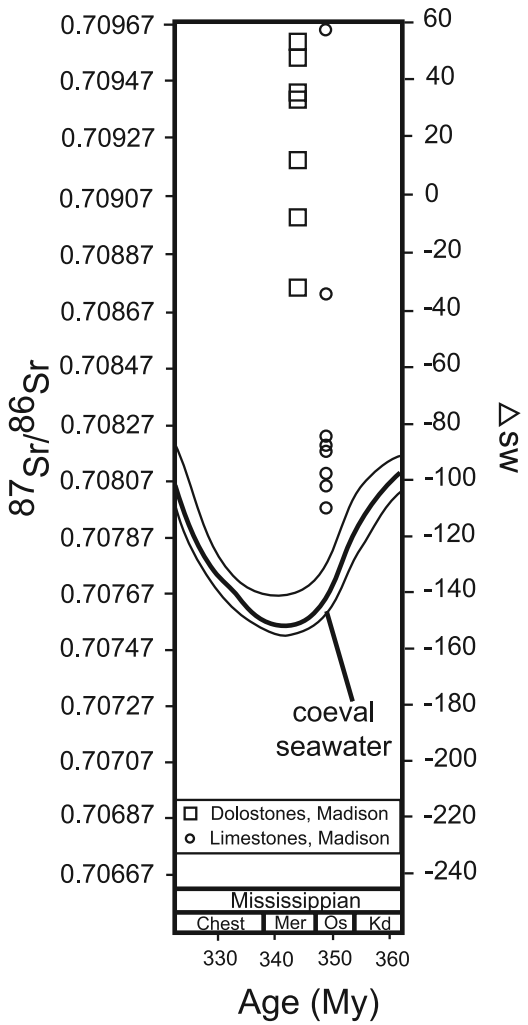

Figure 15. The $^{87}Sr/^{86}Sr$ data from representative carbonate specimens from the study area (modified from *Denison et al.* [1994]). All specimens plot above the band for Mississippian coeval seawater indicating alteration.

from west to east ahead of the deformation as reported by *Enkin et al.* [2000] from the Canadian Cordillera. In addition, a remagnetization trend relative to folding as reported by *Stamatakos et al.* [1996] and *Cox et al.* [2005] from the Appalachians is not evident. We acknowledge that there are not a large number of tilt tests in our study. Extending the study area further west into the disturbed belt could provide additional data to test for the presence of remagnetization trends.

6. Conclusions

[51] The Madison Group carbonates in the Sawtooth Range in Montana contains a widespread late Jurassic–early Tertiary CRM that resides in magnetite. The tilt test results suggest that the CRM was acquired before tilting of the Mississippian Madison Group carbonates in the thrust sheets and Teton anticline and apparently during tilting of the Clary Coulee and Swift Dam folds.

[52] This study aimed to address several issues regarding the origin of the CRM, the difference in timing of the remagnetizations, and the occurrence/lack of remagnetization trends. Petrographic and geochemical studies indicate that the carbonates that contain the CRMs were altered by fluids with elevated $^{87}Sr/^{86}Sr$ values and experienced hydrocarbon migration. Therefore either fluid could have caused the acquisition of the CRM.

[53] The CRMs found in the study area all have the same characteristics. The timing of remagnetization varies from pretilting in the thrust sheets and one fold to syntilting in two of the folds. One possible explanation involves the difference in fold types between the Teton anticline (fault bend fold geometry) and the Clary Coulee and Swift Dam folds (fault propagation fold geometries). It is possible that there was more strain/stress in the Clary Coulee and Swift Dam folds than in the thrust sheets and Teton anticline, which could have modified a magnetization from pretilting to syntilting. A west-east remagnetization trend across the thrust sheets was not observed.

[54] **Acknowledgments.** The authors wish to thank Shannon Dulin, Stephen Osborn, and Crawford Elliott for their assistance on this project. Enormous appreciation is extended to the Blackfeet Indian Reservation in the Swift Reservoir area for allowing the authors to collect field samples. Funding for this project was provided by a grant, DE-FG02-05ER15628, from the Department of Energy to R. D. Elmore and M. H. Engel.

References

Alberta Society of Petroleum Geologists (1964), *Geological History of Western Canada*, 232 pp., Calgary.

Aubourg, C., and C. Chabert-Pelline (1999), Neogene remagnetization of normal polarity in the Late Jurassic black shales from the southern subalpine chains (French Alps): Evidence for late anticlockwise rotations, *Tectonophysics*, *308*, 473–486.

Banerjee, S., R. D. Elmore, and M. H. Engel (1997), Chemical remagnetization and burial diagenesis: Testing the hypothesis in the Pennsylvanian Belden Formation, Colorado, *J. Geophys. Res.*, *102*(B11), 24,825–24,842.

Becker, D. G. (1988), Structural implications of thermal maturity data: Sawtooth Mountains, Montana, M.S. thesis, 136 pp., Univ. of Okla., Norman.

Beske-Diehl, S., and P. N. Shive (1978), The rock magnetism of the Mississippian Madison Limestone, north-central Wyoming, *Geophys. J. R. Astron. Soc.*, *55*, 351–362.

Besse, J., and V. Courtillot (2002), Apparent and true polar wander and the geometry of the geomagnetic field over the last 200 Myr, *J. Geophys. Res.*, *107*(B11), 2300, doi:10.1029/2000JB000050.

Blumstein, A. M., R. D. Elmore, M. H. Engel, C. Elliott, and A. Basu (2004), Paleomagnetic dating of burial diagenesis in Mississippian carbonates, Utah, *J. Geophys. Res.*, *109*, B04101, doi:10.1029/2003JB002698.

Blumstein, R. D., R. D. Elmore, M. H. Engel, J. Parnell, and M. Baron (2005), Multiple fluid migration events along the Moine Thrust Zone, Scotland, *J. Geol. Soc. London*, *162*, 1031–1045.

Borradaile, G. J. (1997), Deformation and paleomagnetism, *Surv. Geophys.*, *18*, 405–435.

Burchfiel, B. C., D. S. Cowan, and G. A. Davis (1992), Tectonic overview of the Cordilleran orogen in the western United States, in *The Geology of North America*, vol. G3, *The Cordilleran Orogen: Conterminous U.S.*, edited by B. C. Burchfiel, P. W. Lipman, and M. L. Zoback, pp. 407–479, Geol. Soc. of Am., Boulder, Colo.

Chamley, H. (1989), *Clay Sedimentology*, 623 pp., Springer-Verlag, Berlin.

Cogne, J. P., and H. Perroud (1987), Unstraining paleomagnetic vectors: The current state of debate, *Eos Trans. AGU*, *68*, 705.

Cox, E., R. D. Elmore, and M. Evans (2005), Paleomagnetism of Devonian red beds in the Appalachian Plateau and Valley and Ridge Provinces, *J. Geophys. Res.*, *110*, B08102, doi:10.1029/2005JB003640.

Denison, R. E., R. B. Koepnick, W. H. Burke, E. A. Hetherington, and A. Fletcher (1994), Construction of the Mississippian, Pennsylvanian and Permian seawater $^{87}Sr/^{86}Sr$ curve, *Chem. Geol.*, *112*, 145–167.

Dolson, J., J. Piombina, M. Franklin, and R. Harwood (1993), Devonian oil in Mississippian and Mesozoic reservoirs—Unconformity controls on migration and accumulation, Sweetgrass Arch, Montana, *Mt. Geol.*, *30*, 125–146.

Dunham, R. J. (1962), Classification of carbonate rocks according to depositional textures, in *Classification of Carbonates Rocks*, edited by W. E. Ham, *AAPG Mem.*, *1*, 108–121.

Dunlop, D. J., and K. S. Argyle (1991), Separating multidomain and single-domain-like remanences in pseudo-single-domain magnetites (215–540 nm) by low-temperature demagnetization, *J. Geophys. Res.*, *96*(B2), 2007–2017.

Elmore, R. D., and L. Crawford (1990), Remanence in authigenic magnetite: Testing the hydrocarbon-magnetite hypothesis, *J. Geophys. Res.*, *95*(B4), 4539–4549.

Elmore, R. D., M. H. Engel, L. Crawford, K. Nick, S. Imbus, and Z. Sofer (1987), Evidence for a relationship between hydrocarbons and authigenic magnetite, *Nature*, *325*, 428–430.

Elmore, R. D., S. W. Imbus, M. H. Engel, and D. Fruit (1993), Hydrocarbons and magnetizations in magnetite, *Spec. Publ. SEPM Soc. Sediment. Geol*, *49*, 181–191.

Elmore, R. D., J. Kelly, M. Evans, and M. Lewchuk (2001), Remagnetization and orogenic fluids: Testing the hypothesis in the central Appalachians, *Geophys. J. Int.*, *144*, 568–576.

Elmore, R. D., J. Foucher, M. Evans, M. Lewchuk, and E. Cox (2006), Remagnetization of the Tonoloway Fm. and Helderberg Gr. in the central Appalachians: Testing the origin of syntilting magnetizations, *Geophys. J. Int.*, *166*, 1062–1076.

Enkin, R. J. (1997), Paleomagnetism data analysis: Version 4.1, Geol. Surv. of Can., Sidney, B. C. (Available at http://www.pgc.nrcan.gc.ca/tectonic/enkin.htm)

Enkin, R. J. (2003), The direction-correction tilt test: an all-purpose tilt/fold test for paleomagnetic studies, *Earth Planet. Sci. Lett.*, *212*, 151–166.

Enkin, R. J. (2004), Paleomagnetism data analysis: Version 4.2, Geol. Surv. of Can., Sidney, B. C. (Available at http://www.pgc.nrcan.gc.ca/tectonic/enkin.htm)

Enkin, R. J., K. G. Osadetz, J. Baker, and D. Kisilevsky (2000), Orogenic remagnetizations in the Front Ranges and Inner Foothills of the southern Canadian Cordillera: Chemical harbinger and thermal handmaiden of Cordilleran deformation, *Geol. Soc. Am. Bull.*, *112*, 929–942.

Evans, M. A., and R. D. Elmore (2006), Fluid control of localized mineral domains in limestone pressure solution structures, *J. Struct. Geol.*, *28*, 284–301.

Fisher, R. A. (1953), Dispersion on a sphere, *Proc. R. Soc. London, Ser. A*, *217*, 295–305.

Gao, G., R. D. Elmore, and L. S. Land (1992), Geochemical constraints on the origin of calcite veins and associated limestone alteration, Ordovician Viola Group, Arbuckle Mountains, Oklahoma, U.S.A., *Chem. Geol.*, *98*, 257–269.

Gill, J. D., R. D. Elmore, and M. H. Engel (2002), Chemical remagnetization and clay diagenesis: Testing the hypothesis in the Cretaceous sedimentary rocks of northwestern Montana, *Phys. Chem. Earth*, *27*, 1131–1139.

Hirt, A. M., W. Lowrie, and O. A. Pfiffner (1986), A paleomagnetic study of tectonically deformed red beds of the Lower Glarus nappe complex, eastern Switzerland, *Tectonics*, *5*, 723–731.

Hoffman, J., and J. Hower (1979), Clay mineral assemblages as low-grade metamorphic geothermometers: Application to the thrust faulted disturbed belt of Montana, U.S.A., *Spec. Publ. Soc. Econ. Paleontol. Mineral.*, *26*, 55–79.

Hoffman, J., J. Hower, and J. L. Aronson (1976), Radiometric dating of time of thrusting in the disturbed belt of Montana, *Geology*, *4*, 16–20.

Hudson, M. R., R. L. Reynolds, and N. S. Fishman (1989), Synfolding magnetization in the Jurassic Preuss Sandstone, Wyoming-Idaho-Utah thrust belt, *J. Geophys. Res.*, *94*(B10), 13,681–13,705.

Jolly, A. D., and S. D. Sheriff (1992), Paleomagnetic study of thrust-sheet motion along the Rocky Mountain front in Montana, *Geol. Soc. Am. Bull.*, *104*, 779–785.

Katz, B., R. D. Elmore, M. Cogoini, M. H. Engel, and S. Ferry (2000), Associations between burial diagenesis of smectite, chemical remagnetization, and magnetite authigenesis in the Vocontian trough, SE France, *J. Geophys. Res.*, *105*(B1), 851–868.

Kent, D. V. (1988), Further paleomagnetic evidence for oroclinal rotation in the central folded Appalachians from the Bloomsburg and Mauch Chunk formations, *Tectonics*, *7*, 749–759.

Kirschvink, J. L. (1980), The least-squares line and plane and the analysis of paleomagnetic data, *Geophys. J. R. Astron. Soc.*, *62*, 699–718.

Kligfield, R. W., W. Lowrie, A. Hirt, and A. W. B. Siddens (1983), Effect of progressive deformation on remanent magnetization of Permian red beds from the Alps Maritimes (France), *Tectonophysics*, *98*, 59–85.

Knechtel, M. M. (1959), Stratigraphy of the Little Rocky Mountains and encircling foothills, Montana, *U.S. Geol. Surv. Bull.*, *1072-N*, 723–752.

Kodama, K. P. (1988), Remanence rotation due to rock strain during folding and the stepwise application of the fold test, *J. Geophys. Res.*, *93*(B4), 3357–3371.

Lageson, D. R. (1987), Structural geology of the Sawtooth Range at Sun River Canyon, Montana Disturbed Belt, Montana, in *Geological Society of America Centennial Field Guide*, edited by S. S. Beus, pp. 37–39, Rocky Mt. Sect., Geol. Soc. of Am., Denver, Colo.

Lewchuk, M. T., M. Evans, and R. D. Elmore (2003), Synfolding remagnetization and deformation: Results from Palaeozoic sedimentary rocks in West Virginia, *Geophys. J. Int.*, *152*, 66–279.

Lowrie, W. (1990), Identification of ferromagnetic minerals in a rock by coercivity and unblocking temperature properties, *Geophys. Res. Lett.*, *17*, 159–162.

McArthur, J. M., R. J. Howarth, and T. R. Bailey (2001), Strontium isotope stratigraphy: LOWESS Version 3: Best fit to the marine Sr-isotope curve for 0–509 Ma and accompanying look-up table for deriving numerical age, *Journal of Geology*, *109*, 155–170.

McCabe, C., and R. D. Elmore (1989), The occurrence and origin of late Paleozoic remagnetizations in sedimentary rocks of North America, *Rev. Geophys.*, *27*, 471–494.

McCabe, C., R. Sassen, and B. Saffer (1987), Occurrence of secondary magnetite within biodegraded oil, *Geology*, *15*, 7–10.

McCelland-Brown, E. (1983), Palaeomagnetic studies of fold development and propagation in the Pembrokeshire old red sandstone, *Tectonophysics*, *98*, 131–149.

Miller, J. D., and D. V. Kent (1986), Paleomagnetism of the Upper Devonian Catskill Formation from the southern limb of the Pennsylvania Salient: Possible evidence for oroclinal rotation, *Geophys. Res. Lett.*, *13*, 1173–1176.

Moreau, M. G., M. Ader, and R. J. Enkin (2005), The magnetization of clay-rich rocks in sedimentary basins: Low temperature experimental formation of magnetic carriers in natural samples, *Earth Planet. Sci. Lett.*, *230*, 193–210.

Mudge, M. R. (1972), Structural geology of the Sun River Canyon and adjacent areas, northwestern Montana, *U.S. Geol. Surv. Prof. Pap.*, *663-B*, 52 pp.

Mudge, M. R. (1982), A resume of the structural geology of the Northern Disturbed Belt, northwestern Montana, in *Geologic Studies of the Cordilleran thrust belt*, edited by R. B. Powers, pp. 91–122, Rocky Mt. Assoc. of Geol., Denver, Colo.

Mudge, M. R., and R. L. Earhart (1983), Bedrock geologic map of part of the northern Disturbed Belt, Lewis and Clark, Teton, Pondera, Glacier, Flathead, Cascade, and Powell counties, Montana, *U.S. Geol. Surv. Map*, *I-1375*.

Mudge, M. R., W. J. Sando, and J. T. Dutro Jr. (1962), Mississippian rocks of Sun River Canyon area, Sawtooth Range, Montana, *AAPG Bull.*, *46*, 2003–2018.

Nichols, K. M. (1980), Depositional and diagenetic history of porous dolomitized grainstones at the top of the Madison Group, Disturbed Belt, Montana, in *Paleozoic Paleogeography of the West-Central United States*, edited by T. D. Fouch and E. R. Magathan, pp. 163–173, Rocky Mt. Sect., Soc. of Econ. Paleontol. and Mineral., Denver, Colo.

O'Brien, V. J., R. D. Elmore, M. H. Engel, and M. A. Evans (2006), Timing and origin of orogenic remagnetizations in Mississippian carbonates, Sawtooth Range, Montana, *J. Geochem. Explor.*, *89*, 297–301.

Oliver, J. (1992), The spots and stains of plate tectonics, *Earth Sci. Rev.*, *32*, 77–106.

Pasternack, I. (1988), Nature and distribution of Mississippian Sun River Dolomite porosity, west flank of the Sweetgrass Arch, in *Rocky Mountain Association of Geologists Carbonate Symposium*, edited by R. B. Powers, pp. 129–138, Rocky Mt. Assoc. of Geol., Denver, Colo.

Pullaiah, G., E. Irving, K. L. Buchan, and D. J. Dunlop (1975), Magnetization changes caused by burial and uplift, *Earth Planet. Sci. Lett.*, *28*, 133–143.

Shipunov, S. V. (1997), Synfolding magnetization: Detection, testing and geological applications, *Geophys. J. Int.*, *130*, 405–410.

Sloss, L. L., and W. M. Laird (1945), Mississippian and Devonian stratigraphy of northwestern Montana, *U.S. Geol. Surv. Oil Gas Invest. Prelim. Chart*, *15*.

Stamatakos, J., and A. M. Hirt (1994), Paleomagnetic considerations of the development of the Pennsylvania Salient in the central Appalachians, *Tectonophysics*, *231*, 237–255.

Stamatakos, J., and K. P. Kodama (1991a), Flexural folding and the paleomagnetic fold test: An example of strain reorientation of remanence in the Mauch Chunk Formation, *Tectonics*, *10*, 807–819.

Stamatakos, J., and K. P. Kodama (1991b), The effects of grain-scale deformation on the Bloomsburg Formation pole, *J. Geophys. Res.*, *96*(B11), 17,919–17,933.

Stamatakos, J., A. M. Hirt, and W. Lowrie (1996), The age and timing of folding in the Central Appalachians from paleomagnetic results, *Geol. Soc. Am. Bull.*, *108*, 815–829.

van der Pluijm, B. A. (1987), Grain-scale deformation and the fold test: Evaluation of synfolding remagnetization, *Geophys. Res. Lett.*, *14*, 155–157.

Van der Voo, R., J. A. Stamatakos, and J. M. Pares (1997), Kinematic constraints on thrust-belt curvature from syndeformational magnetizations in the Lagos del Valle Syncline in the Cantabrian Arc, Spain, *J. Geophys. Res.*, *102*(B5), 10,105–10,119.

Waldhöer, M., and E. Appel (2006), Intersections of remanence small circles: New tools to improve data processing and interpretation in palaeomagnetism, *Geophys. J. Int.*, *166*, 33–45.

Watson, G. S., and R. J. Enkin (1993), The fold test in paleomagnetism as a parameter estimation problem, *Geophys. Res. Lett.*, *20*, 2135–2137.

Zijderveld, J. D. A. (1967), A. C. demagnetization of rocks: Analysis of results, in *Methods in Paleomagnetism*, edited by D. E. Collinson et al., pp. 254–286, Elsevier Sci., New York.

R. D. Elmore, M. H. Engel, K. M. Moreland, and V. J. O'Brien, School of Geology and Geophysics, University of Oklahoma, 100 E. Boyd Street, Norman, OK 73019, USA. (delmore@ou.edu; obrienvj@alumni.ou.edu)

M. A. Evans, Department of Physics and Earth Sciences, Central Connecticut State University, New Britain, CT 06050, USA.